View metadata, citation and similar papers at core.ac.uk

brought to you by CORE

provided by University of East Anglia digital repository

Downscaling regional climate model outputs for the Caribbean using a weather generator

P.D. Jones[1,2]

C.Harpham[1]

A.Burton[3]

and

C.M.Goodess[1]

[1]Climatic Research Unit

School of Environmental Sciences

University of East Anglia

Norwich

NR4 7TJ, UK

[2]Center of Excellence for Climate Change Research / Dept of Meteorology

King Abdulaziz University

Jeddah, Saudi Arabia

[3]School of Civil Engineering and Geosciences

Newcastle University

Newcastle-upon-Tyne

NE1 7RU, UK

Abstract

Locally relevant scenarios of daily weather variables that represent the best knowledge of the present climate and projections of future climate change are needed by planners and managers to inform management and adaptation decision making. Information of this kind for the future is only readily available for a few developed country regions of the world. For many less-developed regions, it is often difficult to find series of observed daily weather data to assist in planning decisions. This study applies a previously developed single-site Weather Generator (WG) to the Caribbean, using examples from Belize in the west to Barbados in the east. The purpose of this development is to provide users in the region with generated sequences of possible future daily weather that they can use in a number of impact sectors. The WG is first calibrated for a number of sites across the region and the goodness of fit of the WG against the daily station observations assessed. Particular attention is focussed on the ability of the precipitation component of the WG to generate realistic extreme values for the calibration or control period. The WG is then modified using Change Factors (CFs) derived from Regional Climate Model (RCM) projections (control and future) to simulate future 30-year scenarios centred on the 2020s, 2050s and 2080s. Changes between the control period and the three futures are illustrated not just by changes in average temperatures and precipitation amounts, but also by a number of well-used measures of extremes (very warm days/nights, the heaviest 5-day precipitation total in a month, counts of the number of precipitation events above specific thresholds and the number of consecutive dry days).

1. Introduction

Assessments of the influence of weather variability on an impact sector (e.g. agriculture and water resources etc.) require observational weather data and an impact model that relates this variability to the impact sector (e.g. crop growth, rainfall/runoff models etc.). For the future, researchers in these impact sectors want to continue to use similar impact models to assess how a changed future climate might affect their sector. There are three major sources of uncertainties that need to be addressed in these studies (see e.g. Parry et al., 2007): uncertainties in the impacts models, in the future climate projections (from General

Circulation Models, GCMs and RCMs) and finally in the way the latter are further 'downscaled' to the relevant space and time scales for the sector. This paper does not consider the first uncertainty, which will be both sector and region specific (Parry et al., 2007). The relative importance of the three uncertainties generally depends on the researcher's perspective, but from a climatic perspective the second should be considered the most important particularly for more distant futures. This paper addresses the third of these uncertainties but it is necessary to consider this in conjunction with the second and in many respects it is difficult to separate the third from the second type of uncertainty.

Due to differences in spatial scales, limitations to process modelling and biases in GCMs and RCMs, some form of downscaling (both in the temporal as well as the spatial domain) is necessary for many impact assessments (Jenkins et al., 2014). Accordingly, researchers have employed a variety of approaches to provide what is the basic requirement: future sequences of weather for a particular time horizon and emissions scenario. Two basic approaches to downscaling have been recognized: statistical and dynamical. Dynamical downscaling concerns the nested simulation of an RCM conditioned by a GCM, whilst statistical downscaling uses empirical relationships between local and larger spatial scales to downscale climate model projections (see Schmidli et al., 2007 for a brief review and an intercomparison of both approaches; Christensen et al., 2007, 2013 for a focus on dynamic downscaling and Maraun et al., 2010 and Wong et al., 2014 for downscaling of precipitation). Traditionally there was a clear distinction between the two approaches. This distinction, however, has become blurred in recent years with the recognition that RCM output should generally not be used directly so that even high-resolution RCM output (at say the 25km resolution and daily timescale) is not sufficiently detailed or still contains biases for direct application to some impact sectors. Thus methods applying statistical downscaling to RCM outputs combining the benefits of both approaches have been developed (e.g. Burton et al., 2010).

A popular type of statistical downscaling methodology concerns the use of a stochastic weather generator (WG) to simulate scenarios of weather that match important statistical properties of known observations. WGs have a long history, extending back to Richardson (1981) when they were first developed for the daily timescale. This WG (WGEN, see also

Richardson and Wright, 1984) developed daily series of precipitation amounts, mean temperature and solar radiation. The original aim was to use the generated sequences to drive a crop-climate model and this is still the use to which most WG outputs around the world are put (Semenov and Barrow, 1997, Zhang, 2005). Improved types of WGs have been developed since the early 1980s (e.g. LARS-WG, Racsko et al., 1991 and CLIGEN, Nicks et al, 1995, see discussion in Chen et al., 2012) and more recently (e.g. EARWIG, Kilsby et al., 2007). The first attempts to modify the output of WGs for their use in studies of future climate impacts were undertaken by Wilks (1992) and also by Katz (1996). Wilks and Wilby (1999) and Wilks (2010, 2012) provide comprehensive reviews of WGs and WG use. The references in these latter two papers show how the use of WGs has extended from crop-climate modelling to other sectors (e.g. rainfall/runoff modelling and building design) and also towards the more direct use of the output in estimating changes in extremes at single sites. It will be this latter direct use that we will illustrate in this paper.

Robock et al. (1993) was one of the first papers to discuss how climate scenarios should be developed from various possibilities (past warm periods, spatial analogues, modifying historic series to GCM output). Their recommendation was to use GCMs as they were the only approach that could produce consistency across multiple climate variables, but there was a mismatch in scales between point observations and the large grid-box sizes of GCMs. WGs provide a relatively simple way to bridge these differences in spatial scales. There are two recognized approaches to modifying WG parameters (Wilks, 2010). The first uses day-to-day changes in parameters according to daily variations in the atmospheric circulation (e.g. Wilby et al. 2002). The second, and much more common approach, has been to modify WG parameters using calculations from GCMs or more recently RCMs (see possible formulations in Wilks, 2010). Initial modification of WG parameters used monthly means and variances of precipitation and temperature, with different values for days that were wet or dry. The use of changes projected by climate models instead of absolute projected climate properties has begun to be referred to as the Change Factor (CF) approach (see Kilsby et al., 2007; Chen et al., 2012). For example, the traditional *perturbation approach* (e.g. Prudhomme et al., 2002) may concern the application of change factors to adjust the mean rainfall properties of observed rainfall records to yield a future rainfall scenario. As daily precipitation generation has become much more complex than the Markov-Chain

approach of Richardson and Wright (1984), CFs encompassing the proportion of dry days, skewness and autocorrelative properties of precipitation have been additionally estimated from GCM, and increasingly RCM, output for application to WGs (e.g. Burton et al., 2010).

Kilsby et al. (2007) illustrate how RCM projections of change (using CFs) can be applied to present day weather statistics (derived from daily observations from a single series) to provide an estimate of the important characteristics of a downscaled future scenario. Subsequently both present day and future scenarios are simulated using the weather generator for a specific location. This approach was updated and further developed to provide future climate scenarios for 5km grid squares across the UK for emulated projections from a perturbed physics ensemble for the UKCP09 national scenarios (Jones et al., 2010). Within UKCP09, one hundred 30-year sequences of daily weather are generated for both the control and future climate. Each of these sequences should be run through the climate-impact model in the sector of interest, or all assessed directly (e.g. for extremes), providing ranges of uncertainty (which encompass the uncertainty of both the WG, the CFs and where used, the impact model). This type of application will be illustrated in this paper for the Caribbean by assessing changes in daily precipitation and temperature extremes at single sites across the region.

The Caribbean region contains more than 20 autonomous states at various stages of economic development. However, regional institutions and national infrastructure planners and resource managers face common practical and political challenges concerning the evaluation of present and future weather-derived resources and hazards. These include the limited availability of observed meteorological datasets and the requirement for locally relevant unbiased downscaled future climate scenarios of weather. Whilst detailed RCM-based downscaling studies have been carried out (e.g. Centella-Artola et al., 2015) and downscaled GCM scenarios are available based on broad brush global scale approaches (Mitchell et al., 2004), a regionally relevant approach taking advantage of both stochastic WG and deterministic dynamical downscaling methodologies is not yet available for this region.

In this paper the need for present and future locally-relevant and unbiased scenarios of weather for locations in the Caribbean is addressed by adapting and evaluating the Kilsby et al. (2007) and UKCP09 (Jones et al, 2010) CF+WG approaches for the region. In particular, care is taken to make the best use of available observed datasets. The WG is fitted to observed daily station data and perturbed using the CF approach applied to recent RCM projections of control and future scenarios for the region. Perturbing the WG in this way provides future weather sequences, which can be used with sector-specific impact models. The approach is assessed by comparing daily control scenarios with available observations. Future climate change is evaluated in terms of changes to both climatology and extreme weather occurrences. Uncertainty due to weather variability is modelled by the multiple simulations of the WG for the current and the chosen future.

The paper is structured as follows. Section 2 discusses the availability of the needed daily climate series across the Caribbean for WG calibration. This section includes some necessary pre-processing and analysis steps as some variables do not appear to be measured in the region, as well as the estimation of important additional variables calculated from the measured weather variables [Potential Evapotranspiration, (PET) and Direct and Diffuse Radiation]. Section 3 introduces the daily version of the WG and illustrates the results of fitting the WG to these data series, together with projections for the future, which is the main aim of this paper. This section additionally discusses the results in the context of extremes in the generated weather sequences. Section 4 concludes. To keep the text relatively short, daily station data availability, the mathematical detail of the WG and the perturbation procedure have all been removed to Appendices.

2. The Caribbean Region and available data

2.1 The climatology of the Caribbean region

The Caribbean Sea is located between 10° and 24°N and exhibits a humid and maritime tropical climate. The Inter-Tropical Convergence Zone (ITCZ) reaches its furthest northward extent in western parts in July and lies across northern South America in December. In the southern parts of the Caribbean region this results in two wet seasons separated by two dry seasons, but centrally and further north there is only a single wet season. The oceanic

setting of the islands in the region results in relatively stable year round temperatures, with average daily temperature range exceeding the magnitude of the seasonal cycle. Across the region the dry seasons are not totally dry, and might be better expressed as being less wet.

The basic climatology of the region has been described in detail by Taylor and Alfaro (2005). Many studies discuss the regional climatology in the context of the hurricanes which periodically cross the region during the June to November season (see the recent paper by Jones et al., 2015). Despite the hurricane season, many studies separate the year into three seasons: May to July, August to October and November to April, although the seasonal breakdown varies across the large region. The irregular occurrence of hurricanes potentially distorts climate statistics, and the effects of this will be discussed later.

2.2 Observed meteorological data

The Jones et al (2010) daily WG requires the following six observed daily meteorological variables in order to be fully calibrated: Precipitation; Temperature minimum; Temperature maximum; Sunshine hours; Vapour pressure (VP); and Wind speed. Although VP is measured directly using a wet-bulb thermometer, it is generally reported as a Relative Humidity (RH) measurement. This is the case for the Caribbean, so it has been necessary to use RH and temperature to recalculate the VP value, as VP is the preferred humidity variable within the WG and is required for the subsequent PET calculation. At some sites across the Caribbean, RH and occasionally sunshine and wind speed are not measured at some of the sites. As these are required for full use of the WG, possible solutions to this problem are discussed in section 2.3.

WG calibration requires at least 20 years of data within a 30-year base period for each month and each year must contain at least 66% of data for that month. Traditionally a 1961-1990 baseline period was used in Europe, however, to maximize the utility of available station datasets, three candidate baselines were evaluated for their coverage of the Caribbean region: 1961-1990; 1971-2000; 1981-2010. Data sparsity in the first period led to it being rejected. The latter two periods were considered, therefore, to be most relevant for the region in terms of historic data completeness and to provide a regional coverage that accepts recently installed observation sites. Figure 1 maps the sites across the Caribbean and Appendix 1 provides a brief regional overview of the 42 most suitable datasets available

for this study together with details of any pre-processing and percentage completeness for each variable. For all Caribbean sites, extreme precipitation values were checked using the HURDAT dataset of hurricane tracks (Knapp et al., 2010) and also reports of extreme rainfall events on Wikipedia.

2.3 Evaluation of / Alternative methods of evaluating VP

The WG was developed for the UK where the length and coverage of daily weather data is more widespread than in the Caribbean. In the rest of this section we discuss and develop the compromises required to enable the WG to be run in a similar way as for the UK. Estimating daily PET requires data for five of the six meteorological variables (temperature mean (average of max and min), sunshine, wind speed and vapour pressure). However, only three Caribbean stations (Philip Goldson International Airport in Belize; Melville Hall, Dominica; and Grantley Adams International Airport, Barbados) to which we have access have an adequate record of daily RH measurements, from which VP may be calculated. All other stations do not appear to measure RH: at least in the archives we are aware of in the region (see Appendix 1 which includes the sources of the observational data).

For two of these sites, we have used RH to calculate VP required by the Penman-Monteith approach for the calculation of PET (see Ekström et al., 2007 for details of this FAO recommended method). This is a simple direct calculation which additionally uses the saturation vapour pressure of the air at the average daily temperature (estimated from the mean of maximum and minimum daily temperature). Alternatively, VP can be estimated from minimum temperature measurements which are available at all sites listed in Appendix 1. The relevant formula is given by Harris et al. (2014, their Equation A7) and also New et al. (1999), where daily minimum temperature is used as a surrogate estimate of dew point temperature. This is an approximation, so here, we use this relationship for two of the sites with vapour pressure measurements and compare the direct and approximated vapour pressure measurements as well as the resulting estimates of PET.

Figure 2 shows the results for the Philip Goldson Airport site in Belize (B5) and Figure 3 for the site in Dominica at Melville Hall (W2). Greater emphasis should be placed on the Belize results as these are based on almost complete daily observations for all variables for the

1981-2010 period. For the site in Dominica, the completeness of the record is poorer. Estimating vapour pressure from minimum temperature has very little effect on monthly PET estimation at the site in Belize. For the site in Dominica, the vapour pressure estimation results in higher values than those measured. For the PET calculation this results in lower estimates than those for PET using the measured vapour pressure values. At both sites the annual cycle of vapour pressure and PET is well produced when comparing the estimates of PET with the direct measurements of VP and those using the formula with minimum temperature. We thus use this relationship between Tn and VP across the region to derive daily VP values where VP or RH are not directly measured.

A few of the Caribbean sites listed in Appendix 1 are additionally missing either sunshine or wind speed measurements or both. For such cases the Penman-Monteith PET calculation cannot be used, so a much simpler approach to PET calculation, developed by Thornthwaite (1948) based solely on temperature measurements, has been used. This development took place over the eastern United States in a region that can be considered a humid climate, somewhat similar to that experienced over much of the Caribbean. A number of papers have compared various PET approaches (including Penman-Monteith and Thornthwaite) in different parts of the world (e.g. Xu and Singh, 2001 and Lu et al., 2005) using measurements made by evaporation pans as the truth. In general, Thornthwaite overestimates PET compared to both the pans and Penman-Monteith in humid climates and underestimates in arid climates (see Pereira and Camargo, 1989), and so adjustment factors have been devised to correct for this (Bautista et al., 2009). We have evaluated the Thornthwaite PET estimate compared to the Penman-Monteith PET (not shown) but although the approach appears reasonable it does not produce the annual cycle of PET shown in Figures 2 and 3. The Thornthwaite approach leads to a slight peak in July, instead of the slightly bimodal distribution evident in Figures 2 and 3. This comes about from the peak in temperatures in July and the Thornthwaite approach being solely based on temperature. Higher humidity values result in slightly lower PET estimates in the high summer months as in the example for Dominica.

Appendix 1 contains a list of the data completeness for each site, including sites where VP has been estimated from Tn. At one of the sites on Barbados, sunshine measurements have

been used from a nearby site to produce a more complete record. Full details of this are also given in Appendix 1. Users wanting access to the raw station need to contact the appropriate Meteorological Service.

2.4 Available Climate model projections

Relatively high resolution, 25km, Caribbean region future climate scenario projections were available for use in this study over the projection time-domain 1961-2100 for the A1B SRES emissions scenario (Taylor et al., 2007; Centella-Artola et al., 2007; Campbell et al., 2010; Karmalkar et al., 2013; Centella et al., 2014). These projections were produced by the dynamic downscaling of the HadCM3Q0 and ECHAM5 GCMs to 25km resolution using the PRECIS RCM (for model details see Centella-Artola et al., 2015). Projections for the 2020s (2011-40), the 2050s (2041-70) and the 2080s (2071-2100) were used in this study together with the RCM run for the control-run period of 1981-2010. The projections developed in this study, therefore, are based on just two GCM/RCM combinations, so will not fully sample the uncertainty range. To undertake such an exercise, users would need to apply similar or different methodologies to the WG but with an extended range of GCM/RCM combinations which are becoming available within the CORDEX initiative (see for example for the North American Domain in Martynov et al., 2013) This study does also not assess how well hurricanes are simulated by the RCMs, but it discusses how hurricanes might distort the precipitation series.

Many more GCM simulations are available for this region and are discussed in the latest Intergovernmental Panel on Climate Change (IPCC) Report by Christensen et al. (2013, see also the Atlas Annex available at https://www.ipcc/report/ar5/wg1). Here 39 GCMs are averaged in the Coupled Model Intercomparison Project 5 (CMIP5) across the Caribbean and Central America in their Figure 14.19 [for the median Representative Concentration Pathway (RCP) 4.5] and compared with 24 GCMs from CMIP3 (from the previous IPCC Report in Christensen et al., 2007). For precipitation, the CMIP5 model average indicates a drying for 2081-2100 with respect to 1986-2005 for the June to September season, with little change evident for the December to March season. For periods nearer the present (we chose 2046-65 for comparison with our 2050s) the average drying for June to August (JJA) is 6% across the 39 GCMs (see Table 14.1 of Christensen et al., 2013). Temperature increases

within the CMIP5 average for this region, also for RCP4.5, are 0.8°C for both December to February (DJF) and JJA. Our two GCMs (HadCM3Q0 and ECHAM5) are consistent with the CMIP5 ensemble average. Later (in section 3.4 and the conclusions), we will bear these average projections in mind when discussing our results for the 2050s.

3. Methodology and application

3.1 The Weather Generator (WG)

WGs have a long history of use in hydrology, climatology and agriculture (e.g. Semenov, 2008; Kilsby et al., 2007; Wilks, 2010, 2012). The WG used here is a development of the EARWIG (Kilsby et al., 2007) and UKCP09 (Jones et al., 2010) WGs for the CARIWIG project http://www.cariwig.org/). The WG was designed to provide unconditional simulations, in the sense that they are independent of external forcing (e.g. by large-scale circulation), for a single location of internally consistent daily time series of meteorological variables: precipitation, temperature (min and max), vapour pressure, wind speed and sunshine. Fitting the CARIWIG-WG requires at least 20 years of data (within one of the 30-year baseline time periods) with simultaneous measurements of all the variables (the completeness of the available data was discussed in section 2.2). The parameterised WG can then generate series at a daily time resolution using two stochastic models in series. First, a model generates precipitation which is subsequently used to condition a second model, which generates the other variables dependent on precipitation. Table 1 details the units and notation for the six generated weather variables and the order in which their simulation is carried out. If observations of a meteorological variable of suitable length are not available, then this variable will be omitted from the fitting and simulation steps of the model. However, the omission of a secondary variable can prevent the simulation of tertiary variables, and the omission of rainfall will prevent the simulation of all variables. Complete details about the structure of the WG used here are provided in Appendix 2. This WG has had usage outside the UK and a summary of applications in Europe is provided by Forsythe et al. (2014) who apply a variant of the WG to the Upper Indus Basin in Pakistan, where there is a climate quite different from the Caribbean.

As shown in Table 1, a number of useful additional meteorological variables may be calculated from the six generated variables: Relative humidity; Potential Evapotranspiration

(PET) (according to the formula given in Ekström et al., 2007); and Diffuse and Direct Radiation (according to the formula given in Muneer, 2004), which for example are particularly important for building design. Provision of these calculated variables supports the impacts community and provides consistency across different impact sectors. If users required PET or the radiation terms for their software application, then self-calculated formulae might be differently produced between sectors. To ensure that users have access to exactly the same data, the derived variables are provided as part of the WG output.

3.2 WG Simulation and Validation of the baseline climate

To fit the CARIWIG WG five statistics of daily rainfall were used to characterise baseline climate: the mean, proportion of dry days (defined as a day with less than 1.0mm of rainfall), variance, skewness and the lag-1 autocorrelation (see Burton *et al.* 2008 for definition of these terms). The lag–1 autocorrelation helps in the fitting of persistent events such as long dry spells. The fitting of the rainfall model and the conditional autoregressive model of the other five meteorological variables are described in Appendix 2.

Preliminary testing of the WG was applied to four of the Caribbean sites: B2 and B5 in Belize and W6 and W7 in Barbados as these had immediate interest from stakeholders. Illustrative examples are shown of analysis of the WG simulations for sites W6 (Husbands in Barbados) and B5 (Philip Goldson Airport in Belize).

Figures 4 and 5 show the fits for the two sites. These plots compare monthly averages for three precipitation variables [PDRY (the dry day proportion), mean daily intensity and the interannual variability of the monthly totals] and maximum and minimum temperature (Figures 4a and 5a) with the other variables (sunshine, wind speed, vapour pressure and PET) shown in Figures 4b and 5b. The calculation of the values for each five panels is straightforward (see also Jones et al., 2011). The interannual variability of monthly precipitation is the standard deviation of the 30 values for each month. In each panel, the value for the observed data (shown in blue) is compared with the range of 100 30-year simulated sequences from the WG (shown in black, with the range showing ± 2 standard deviations of the 30-year averages).

The first aspect of Figures 4 and 5 to compare is that the blue observational plus sign should usually be encompassed by the ±2 standard deviation range of average values from the 100

30-year WG simulations for the same period. This is the case for maximum and minimum temperature and the other non-precipitation variables. For the precipitation variables, the ranges from the WG simulations do not always include the observational value. This occurs very occasionally for PDRY, particularly in November and occasionally in May for Husbands (Figure 4a) and for October and June for the Belize site (Figure 5a).

The issue here appears related to one exceptional daily precipitation event in the observed series in that month – a value much larger than the second and third highest daily precipitation totals. This value may be the result of an exceptional event or it may still be an error in the observed data. If this value is removed the fit is much more acceptable, but we have retained the value when fitting the WG as described in Appendix 2. Extreme observed values in October and November might be related to the passage of a hurricane near the site producing a very high daily precipitation value. As stated, we checked the extreme precipitation values for all Caribbean sites against a dataset of hurricane tracks (Knapp et al., 2010) and also reports of extreme rainfall events on Wikipedia. Extreme daily precipitation values occasionally occur outside of the hurricane season, often in the spring season (particularly April and May) resulting from the passage of cold fronts coming from the northwest (see Taylor and Alfaro, 2005, for a discussion of the climatology of the region). When the WG is fit to the observed data, the assumption is made that all values come from the same distribution. The effect of a hurricane could be considered as something different, more so if only one event occurs during the 1981-2010 period for individual months.

3.3 Estimating Downscaled Future Climate Projections

Projections of downscaled future climate scenarios were estimated using the Kilsby et al. (2007) and Jones et al (2010) CF approach. This approach makes the assumption that the relative change projected to occur in the average properties of RCM simulated meteorological variables is reliable. This assumption is made in almost all applications of GCM and RCM output and is often referred to as the delta approach. Here the future climate is the current climate plus the climate change component (which is the difference between the future and control climate of the RCM or sometimes even the GCM).

Implementation of this approach requires the derivation of change factors (CFs) for each meteorological variable or statistic, as summarized in Table 1 and detailed in Appendix 3.

First, RCM projections downscaled from different driving GCMs were selected, one for each country: HadCM3Q0 for Barbados and ECHAM5 for Belize. Climatologically averaged meteorological variables or statistics were calculated from the PRECIS RCM output for the control period (1981-2010) and for the future scenarios: 2020s (2011-2040) for the Barbados locations and 2050s (2041-2070) for the Belize locations. Typically and in brief, each CF was calculated as the ratio [difference] of the climatologically averaged future scenario variable to the control; then future scenario properties estimated as the product [sum] of the CF with the climatologically averaged control period observation of that variable. Details of the derivation of the CFs is provided in Appendix 3. The choices made here in Figures 4 onwards are just for illustrative purposes. The WG has been run for all three scenario futures, for both driving GCMs and for all 42 sites (http://caribbeanclimateblog.com/2015/02/10/the-caribbean-weather-impact-group-cariwig-project-supports-risk-based-decision-making/ with the generated sequences available on the CARIWIG web site (http://www.cariwig.org/).

3.4 Evaluation of Future climate scenarios

To parameterize the WG for each estimated downscaled future scenario, the precipitation change factors were first applied to the baseline rainfall properties to estimate those of the future scenarios for the two locations that are illustrated in this paper. The rainfall model was then fitted for each scenario and site, and 100 daily simulations of 30-years were simulated. For the remaining variables, the standardisation parameters of the conditioned autoregressive model were perturbed according to the CFs. Finally each rainfall dataset was used to condition the auto-regressive simulation of the remaining variables. Thus for each site and scenario (control and the selected future), a set of 100 30-year long daily timeseries of the six consistent meteorological variables were generated. For further details of the parameterisation of the CARIWIG-WG for the future scenarios see Appendix 3, for details of the fitting of the WG and its simulation, see Appendix 2.

Figures 4a and 5a additionally include the WG simulations for the future precipitation scenarios so these can be compared to both the observations and the WG simulations for the control period. For the Husbands site for the 2020s, PDRY increases in all months except October and precipitation intensities increase between September and December, but

decrease slightly or barely change in the other eight months (Figure 4a). The situation is similar for the Belize site for the 2050s. Here PDRY tends to increase for all months except for October and November (Figure 5a). Precipitation increases occur in October and November, and decrease from April to September. Both results are similar (not shown) if the other forcing GCM is used. Looking further into the future (2080s, not shown) a similar pattern of precipitation change occurs. When compared to other GCM simulations (see the final paragraph of Section 2.4), our two GCMs agree on the drying for the June to August season discussed in Christensen et al. (2013) and also on little change in the overall December to February total. Precipitation increases in October and November are not discussed in Christensen et al. (2013), nor in the Atlas Annex mentioned in Section 2.4.

Related to the earlier discussion about hurricanes, the CF approach used here assumes that the GCMs/RCMs simulate such events regularly and in a similar way and with a similar frequency for both the control and future scenarios as has happened and may happen in the real world. However, the use of two relatively short periods in the calculation of the CFs could give rise to some erratic statistical estimates should outlier events occur in the observational record, or in the RCM control or future scenario. The effect is likely to result in the WG not fitting affected projections well, resulting in greater variability in the different WG sequences. This issue is a potential explanation for the increased variability of WG sequences for some months of the year at the two locations illustrated in this paper.

For temperatures and vapour pressure, all the projections produce increases in the future (Figures 4b and 5b), but by greater amounts for each successive future period (2050s warmer than the 2020s and 2080s warmer than the 2050s, not shown). The temperature increases agree with Christensen et al. (2013) with greater increases for more distant futures (the latter gives 2.8°C for DJF and 3.0°C for JJA by the 2080s). Little change takes place in both locations for sunshine and wind speed, but the latter is not surprising as the changes for wind speed can only occur as a result of changes in precipitation and temperature as no specific CF was calculated for wind speed (as there was little confidence in the wind speed projections for the UK, see Jones et al., 2010). These results are similar for both forcing GCMs used and both locations.

3.5 Evaluation of extremes

Extremes in the observations and WG simulations were characterised in two different ways. The first was to identify days from the 30-year period when precipitation exceeded three fixed thresholds (50, 80 and 150mm) then to partition and count these by calendar month. The results of this are shown in Figures 6 and 7 (as days per month per 30-year period) with the plots structured in a similar way as in Figures 4 and 5: each shows a different site, future period and driving GCM. For the WG simulations, averages and variability are presented (two standard deviations of the 30-year estimates), while for the observations there is just one value calculated from the 1981-2010 baseline. For both sites for the control period, the observational total is within the distribution of the 100 synthetic 30-year sequences. For the Husbands site on Barbados (Figure 6) more heavy precipitation events occur for the 2020s during September to December for the HadCM3Q0 driving GCM. For the 2050s and 2080s (not shown), this increase reduces to just October and November. Results are similar for the ECHAM5-forced sequences (not shown) with the increased counts of precipitation occurring from October to December. For the Belize site (Figure 7), a similar situation occurs with increases in heavy precipitation counts confined to October to November. For the HadCM3Q0-forced sequences (not shown) increases occur for October to December. For the Belize site, the number of extremes exceeds the control period between these months, but the increases reduce from the 2050s to the 2080s.

The second characterisation concerns the use of five extreme indices (see Table 2) chosen from those calculated by software available from the Expert Team on Climate Change Detection and Indices (ETCCDI). This software is available from the ETCCDI website (http://etccdi.pacificclimate.org/software.shtml) and is discussed in Zhang et al. (2011) and used in the Caribbean by Stephenson et al. (2014). These five indices were calculated from the observed station data and compared to the same calculations applied to each of the 100 30-year baseline simulations of the WG. The indices calculated for the simulations were summarized as means and two-standard deviation ranges. Three of the indices (TX90p, TN90p and Rx5day) are calculated for each month of the year, but CDD and R95p are only available as an annual value as their calculation needs to cross monthly and seasonal boundaries. For each set of future scenarios, the 100 future simulations were evaluated as for the baseline simulations, except that the necessary percentile-based thresholds were taken from a control scenario rather than the future scenarios. This choice of threshold

allowed the projected change in extremes to be illustrated against a fixed threshold to assess changes. It was therefore necessary to choose one of the 100 control sequences to provide the basis for the percentile-based thresholds for the future, accordingly this was chosen by proximity to the median annual precipitation total from all 100 30-year simulations.

The results of these analyses for the same GCM/RCM configurations for the Husbands and Philip Goldson site are given in Figures 8 and 9. As expected the number of warm days and nights dramatically increases for the future periods. By definition the value for the observed and the control runs of the WG average to about 10 days in each month over the 30-year period. By the 2080s (not shown) counts above the same monthly thresholds increase to 60-100 days – with the highest values in the late spring and early summer months. The precipitation indices generally decrease slightly in the future, but increase for October to December and also annually as they did with the threshold extremes in Figures 6 and 7. At both sites the number of consecutive dry days also increases slightly in the future periods. For both precipitation extremes (RX5day and R95p), these increases are relatively small compared to the dramatic increases evident for temperatures.

4. Conclusions

The principal aim of this study has been to provide locally-relevant scenarios of daily weather variables in order for impact studies to be undertaken across the Caribbean. The WG sequences are only available at the 42 sites, but further work could enable these to be extended to more sites across the region. The main limiting factor in doing this is the availability, length and completeness of the observational data across the region. If this could be co-ordinated centrally, then much more could have been achieved. A second, but less limiting factor, is that only a limited number of RCM simulations are available for this region, although more are becoming available through the CORDEX project. Some CORDEX simulations are at a coarser resolution (50km) and their scenarios are based on Representative Concentration Pathways as opposed to the emission scenario we have available here. Far more RCM simulations are available for more developed regions like North America and Europe. The more that can be used (in an ensemble type mode as with UKCP09) reduces the risk of the projections leading to poor decisions when based on only a

couple of RCM simulations. The results of this project should be considered with this in mind. Enhancements will come with higher-resolution modelling, but there needs to be better co-ordination of data bases across the region.

In this study we have assessed 42 daily Caribbean weather series that are relatively complete and suitable for providing the basis for impacts studies in the region. Not all the series are complete enough for some of the variables and for most of the sites we have had to estimate Vapour Pressure from minimum temperature across the region. This was necessary to estimate a number of derived variables (such as PET), an essential variable for looking at hydrological impacts in the region. Estimating daily PET requires data for temperature mean (average of max and min), sunshine, wind speed and VP, where the latter is typically estimated from relative humidity measurements. Estimating VP based on minimum temperature was found to lead to a good estimate of Penman-Monteith PET where relative humidity data is unavailable. At some sites, however, sunshine and wind speed measurements are unavailable. For these sites, the Thornthwaite (1948) estimate of PET may provide a reasonable estimate, however, it should be used with caution and correction to this scheme (e.g. Bautista et al., 2009) should be considered.

One aspect of data quality that deserves additional attention is some potentially erroneous daily precipitation totals. The highest precipitation totals for the 42 sites were checked by looking at hurricane tracks and also reports of extreme events on Wikipedia. Related to this, the study has made no specific assessment of possible changes in hurricanes nor does it separate out hurricane-related precipitation from the daily precipitation series. The study has also not assessed how well hurricanes are simulated by the RCMs.

The main outputs of this study are the daily WG sequences for the sites across the region, which can be accessed from the CARIWIG web site, along with guidance and examples of the use of the WG information in specific regional case studies across the Caribbean (publication of these studies is expected in the relevant and sector-specific literature). For each site, there are 100 30-year sequences of weather data for the site's baseline (see Appendix 1) and 100 30-year sequences for each of the three 30-year futures (2020s, 2050s and 2080s) and for two different GCM drivers of the same RCM. For the future simulations, all sites show increases in temperature which become greater for the more distant futures.

This is in agreement with the assessments for the region in Christensen et al. (2013). For precipitation, PDRY increases and precipitation amounts reduce for much of the year, but precipitation intensities increase for the October to November period. Reduced precipitation amounts for June to August are noted in Christensen et al. (2013), but they do not specifically consider October and November. In terms of extremes, warm days and warm nights (temperatures above the current 90th percentiles) increase from 10 per year (by definition) for the control period (1981-2010) to 60-100 per year by the 2080s. Extreme precipitation measures decrease slightly for most months in the future, but increase in October and November suggesting an overall annual increase. Also the number of very wet days are projected to increase. At both sites the number of consecutive dry days also increases in the future periods. For both precipitation extremes, however, the increases are relatively small compared to the dramatic increases evident for temperatures.

Appendix 1: Completeness of daily data series for sites across the Caribbean for two baseline periods (1971-2000 and 1981-2010)

Rainfall extremes >200mm were checked against the HURDAT2 hurricane database (maintained by the National Oceanic and Atmospheric Administration's (NOAA's) National Hurricane Center) to establish if they were genuine.

If maximum temperature was less than minimum temperature then both were set to missing. Wind was converted from knots to m/s.

Relative humidity was multiplied by saturation vapour pressure (calculated from temperature using standard formulae) to give vapour pressure.

There were a few instances in the Cuban data where whole years of rainfall were found to be zero, these were set to missing. To estimate sunshine hours, cloud cover was converted to a decimal fraction, subtracted from one and then multiplied by the day length.

The analysis for Grantley Adams in Barbados made use of sunshine hours recorded at Husbands to enable all the variables to be output.

The Caribbean Institute of Meteorology and Hydrology (CIMH) data contained a few stations which duplicated those provided directly by some National Meteorological Services, so these were removed. A small quantity of temperatures were measured in Fahrenheit which were converted to Celsius. There were also some sunshine hour entries which appeared to be out by a factor of ten, and this was assumed to be the case.

Wind speed and relative humidity data were received (from a few National Meteorological Services in the region) and added to the CIMH data which didn't have any records for these variables.

						1971-2000						1981-2010					
	Station name	Country	Lat (°N)	Long (°W)	Elev (m)	% SS	% TN	% TX	% VP	% WN	% RN	% SS	% TN	% TX	% VP	% WN	% RN
B1	Belmopan	Belize	17.3	-88.8	90	65	73	68	0	37	80	64	88	83	0	62	94
B2	Central Farm	Belize	17.2	-89.0	90	74	92	92	1	87	96	70	98	97	0	99	99
B3	Cooma Cairn	Belize	17.0	-88.9	952	0	66	66	0	0	73						

B4	Melinda Forest Station	Belize	17.0	-88.3	30	22	83	70	0	49	92	36	93	81	0	72	99
B5	Philip Goldson Intl'	Belize	17.5	-88.3	5	89	96	96	60	82	100	98	98	98	87	98	100
C1	Cabo San Antonio, Pinar Del Rio	Cuba	21.9	-85.0	8	86	86	86	0	86	80	89	89	89	0	89	90
C2	Pinar Del Rio	Cuba	22.4	-83.7	37	80	79	79	0	80	80	96	95	95	0	96	96
C3	Bahia Honda, Pinar Del Rio	Cuba	22.9	-83.2	3	96	96	96	0	96	83	100	100	100	0	100	100
C4	Batabano, La Habana	Cuba	22.7	-82.3	7	70	60	60	0	63	66	93	84	84	0	87	90
C5	Punta Del Este, Isla De La Juventud	Cuba	21.6	-82.5	10	93	93	93	0	93	93	100	98	99	0	100	100
C6	Casa Blanca, La Habana	Cuba	23.2	-82.4	50							87	87	87	0	87	87
C7	Playa Giron, Matanzas	Cuba	22.1	-81.0	5	93	93	93	0	93	83	100	90	97	0	100	99
C8	Cantarrana, Cienfuegos	Cuba	21.9	-80.2	42	89	88	88	0	89	89	100	95	94	0	100	100
C9	Jucaro, Ciego De Avila	Cuba	21.6	-78.9	1	96	93	94	0	96	96	100	94	95	0	100	100
C10	Caibarien, Villa Clara	Cuba	22.5	-79.5	6	99	99	99	0	99	99	100	100	100	0	100	100
C11	Sancti Spiritus, Sancti Spiritus	Cuba	21.9	-79.5	97	86	86	86	0	86	83	100	100	100	0	100	100
C12	Santa Cruz Del Sur, Camaguey	Cuba	20.7	-78.0	2	84	82	84	0	84	84	87	86	85	0	87	87
C13	Nuevitas, Camaguey	Cuba	21.5	-77.3	4	96	96	96	0	96	96	99	99	99	0	99	99
C14	Camaguey	Cuba	21.4	-77.9	122	100	100	100	0	100	100	100	100	99	0	100	100
C15	Puerto Padre, Las Tunas	Cuba	21.2	-76.6	13	96	92	92	0	96	96	100	96	97	0	100	100
C16	Cabo Cruz, Granma	Cuba	19.9	-77.2	10	100	99	99	0	100	100	100	99	100	0	100	100
C17	Contramaestre, Santiago De Cuba	Cuba	20.3	-76.3	100	81	78	78	0	67	61	100	100	100	0	100	83
C18	Punta Lucrecia, Holguin	Cuba	21.1	-75.6	4	98	96	96	0	98	98	99	99	99	0	99	99
C19	Punta De Maisi, Guantanamo	Cuba	20.3	-74.2	10	72	71	71	0	72	72	100	98	99	0	100	100
J1	Worthy Park	Jamaica	18.2	-77.2	550	0	85	81	0	0	74	0	90	87	0	0	82
A1	Vc Bird Intl' Airport	Antigua	17.1	-61.8	14	0	91	91	86	98	98						
W1	Nat. Agric. Station	St. Kitts	17.3	-62.2	0							0	84	84	0	0	85
W2	Melville-Hall	Dominica	15.6	-61.3	43	63	62	62	37	67	85	83	91	91	37	67	96
W3	Canefield	Dominica	15.3	-61.4	4							0	67	67	0	0	67

W4	Roseau	St. Lucia	13.9	-61.0	0	67	68	67	0	0	68						
W5	Hewannorra	St. Lucia	13.8	-61.0	21	32	72	72	0	0	81	35	87	87	0	0	96
W6	Husbands	Barbados	13.2	-59.6	112	98	99	98	0	0	100	98	99	99	58	60	100
W7	Adams	Barbados	13.1	-59.5	35							0	98	98	98	98	100
W8	ET Joshua Airport	SVG	13.1	-61.2	13							0	80	80	46	45	80
W9	Point Salines	Grenada	12.2	-61.8	0							0	79	78	0	0	79
W10	Crown Point	Tobago	11.2	-60.8	3	94	91	91	0	0	92	84	81	81	0	0	81
W11	Piarco	Trinidad	10.6	-61.4	41	96	93	93	0	0	93	92	89	89	0	0	89
W12	St. Augustine	Trinidad	10.6	-61.4	16	95	95	95	0	0	95	100	99	99	0	0	99
W13	Georgetown Bot. Gardens	Guyana	6.8	-58.1	0	86	99	99	0	0	100	96	99	98	0	0	100
W14	Timehri Airport E.B.D	Guyana	6.5	-58.3	3	15	74	75	0	0	100	33	71	71	0	0	98
W15	New Amsterdam Tecn Ins	Guyana	6.2	-57.5	0							54	74	71	0	0	90
W16	Ebini Livestock Station	Guyana	5.6	-57.8	0	15	72	66	0	0	76	39	73	69	0	0	79

Dataset sources are indicated as follows: B*i* from the Belize National Meteorological Service ; C*i* from the Cuban Instituto de Meteorologia; J*i* from the Jamaican Meteorological Service; A*i* from the Antigua and Barbuda Meteorological Service ; and W*i* from CIMH. Please see *Acknowledgements* for further details.

Appendix 2: The CARIWIG Weather Generator (WG)

Most weather generators generally take rainfall to be the primary variable (Wilks and Wilby, 1999; Wilks, 2010), so that other weather variables are conditioned by mathematical/statistical relationships with rainfall and the values of the variables on the current and previous day. The CARIWIG-WG also maintains the autocorrelation properties of each variable as well as the cross-correlations between the different variables, producing sequences that look like and statistically resemble measured data. Collectively these auto- and cross-correlation relationships are referred to as the *inter-variable relationships* (or IVRs). Apart from the daily autocorrelation of precipitation, none of these IVRs are perturbed for future scenario simulations of the WG as they are not considered well simulated by RCMs.

A2.1 The rainfall model

Rainfall is modelled according to a Neyman-Scott Rectangular Pulses (NSRP) stochastic process (e.g. see Cowpertwait *et al.* 1996; Burton et al., 2008), one of a family of long-established point process models (see Velghe *et al.* 1994 and Onof *et al.* 2000 for overviews). This process models the timing and intensity of rainfall as rain-bearing raincells which are clustered into storms. Here a variant of the NSRP model is used in which the intensity of the raincells is modelled with a Gamma distribution, considered particularly suitable for modelling extremes which in the Caribbean climate may include tropical storm events.

The model structure and its six parameters may be summarized as follows:

1. storm origins arrive in a Poisson process with rate parameter λ (h^{-1});
2. each storm origin generates a random number [Poisson distribution with parameter v (-, i.e. dimensionless)] of raincells each following the storm origin after a time interval (exponentially distributed with parameter β (h^{-1}));
3. the duration of each raincell is exponentially distributed with parameter η (h^{-1});
4. the intensity of each raincell has a Gamma distribution (with shape parameter K (-) and scale parameter θ (mm/h));

5. the rainfall intensity is equal to the sum of the intensities of all the active cells at that point.

Aggregation of the intensity process over regular time steps, here daily, yields (daily) accumulation time series. The model parameters may differ for each month of the year to provide seasonality, and accordingly model fitting proceeds on a monthly basis. Analytical expressions have been derived for expected values of various rainfall statistics (e.g. mean rainfall rate, proportion of dry days) in terms of these model parameters, and these are used to numerically fit sets of parameter values by minimizing a measure of the expected and observed values of a set of rainfall statistics. Robust and accurate fits to the lower order moments (mean, variance) are generally obtained, and much development has been carried out to improve the model performance for rainfall occurrence, and extremes using the skewness in fitting. Note that although the raincell intensity in Step 4 follows a Gamma distribution, the daily accumulations may arise from multiple overlapping raincells in a cluster.

A2.2 Secondary and tertiary weather variables

Once the precipitation sequence has been simulated, the secondary and tertiary daily meteorological variables (Table 1) are modelled using a conditional multivariate autoregressive approach. This maintains the IVRs and their conditioning by both the seasonal cycle and the simulated rainfall. The precipitation model is developed separately for each month of the year, with the secondary and tertiary variables also developed for each month of the year. Both models are based on the same calibration period (which is discussed for each site in the region in Appendix 1).

The model structure for daily temperature considers a transformed pair of daily quantities to generate the secondary variables: the mean temperature defined as $T = (Tn + Tx)/2$; and the diurnal temperature range defined as $R = Tx - Tn$. Note that the secondary variables may be recovered by the inverse transformations: $Tx = T + R/2$ and $Tn = T - R/2$. Within each calendar-month partition, the transformed multi-variate dataset is further partitioned by wet (W) and dry (D) daily rainfall transition states [where five rainfall transitions DD, DDD, WW, DW and WD are considered, in each case the final letter indicating the current day's state and preceding letter(s) indicating antecedent state(s)]. Rather than directly modelling

the seasonally changing meteorological variables, the variables *T* and *R*, are first standardised by subtracting the mean and dividing by the daily standard deviation of each variable within each calendar month and rainfall transition partition. VP and sunshine duration (S) were treated similarly, but the means and standard deviations were calculated overall and not for each rainfall transition. For S, however, the Kilsby *et al.* (2007) standardisation procedure was modified here, as this variable is often not normally distributed as is required for an auto-regressive approach. Instead, a latent Gaussian variable technique (Durban and Glasbey, 2001) was applied to each month where the input variable is transformed to the upper part of a Gaussian distribution, the lower part (i.e. below a threshold) of the same distribution is considered to correspond to zero sun days.

For both daily mean temperature and range, the residual time series are modelled as first-order autoregressive processes, the IVRs, which are assumed not to change in the future. A different model structure being used for each rainfall transition state as follows (note that all terms are standardised here):

Transition state DD, i.e. current day dry, previous day dry:

$$T_i = a_1 T_{i-1} + a_2 S_{i-1} + b_1 + \varepsilon_1 ; \quad R_i = a_3 R_{i-1} + a_4 S_{i-1} + b_2 + \varepsilon_2 ;$$

Transition state DDD, i.e. current day dry, previous two days dry:

$$T_i = a_5 T_{i-1} + a_6 S_{i-1} + b_3 + \varepsilon_3 ; \quad R_i = a_7 R_{i-1} + a_8 S_{i-1} + b_4 + \varepsilon_4 ;$$

Wet Periods (WW current day wet, previous day wet):

$$T_i = a_9 T_{i-1} + b_5 + \varepsilon_5 ; \quad R_i = a_{10} R_{i-1} + b_6 + \varepsilon_6 ;$$

Dry/Wet Transition (DW current day wet, previous day dry)

$$T_i = a_{11} T_{i-1} + a_{12} P_i + b_7 + \varepsilon_7 ; \quad R_i = a_{13} R_{i-1} + a_{14} P_i + b_8 + \varepsilon_8 ;$$

Wet/Dry Transition (WD current day dry, previous day wet)

$$T_i = a_{15} T_{i-1} + a_{16} P_{i-1} + b_9 + \varepsilon_9 ; \; R_i = a_{17} R_{i-1} + a_{18} P_{i-1} + b_{10} + \varepsilon_{10} .$$

The coefficients $\{a_1, ..., a_{18}, b_1, ..., b_{10}\}$ may be fitted using multiple linear regression analysis of standardised observed data, the suffix *i* and *i* -1 indicating the current day and previous

day respectively, and the error terms, ε_1 ... ε_{10}, are independent standard normal (Gaussian) variables to model the unexplained variance of each regression. In simulation, i.e. weather generation mode, these auto-regressive processes are realized by sampling the error terms. To help improve modelling accuracy of dry day sequences, the antecedent sunshine-hours term was included in the temperature models for the DD and DDD partitions. DDD was incorporated into the most recent update of UKCP09 (Jones et al., 2010).

The tertiary variables are modelled using a conditional first order auto-regressive process of the form:

$$X_{j,i} = c_j + d_j P_i + e_j T_i + f_j R_i + g_j X_{j,i-1} + \varepsilon_{10+j}$$

where: j = 1,2 indicates vapour pressure and sunshine duration: coefficients *c*,*d*,*e*,*f* and *g* are fitted for each month and an error term, ε, is also required in each case. Correlations between the tertiary variables and precipitation, temperature and temperature range (which are generally quite high) will also be correctly simulated, and correlations between vapour pressure, sunshine and wind speed will arise naturally through common dependencies on P_i, T_i and R_i. Fitting of the tertiary models is achieved by multi-variate regression. The fully fitted non-rainfall part of the WG results in many thousands of parameters, which include: the means and standard deviations for each half month for each transition for *T* and *R*; and the regression coefficients and magnitude of the random error components in the conditioned autoregression equations.

Simulation of the secondary and tertiary variables starts with a conditioning rainfall series, then proceeds by simulating the variables one day at a time using the autoregressive relationships as selected by the current month and rainfall transition partitions, antecedent variables, conditioning variables and random sampling of the random error term. Finally all the variables are transformed back from their standardised representations. Projections produced using RCMs for wind were not considered reliable in the UK (Jones et al., 2010, 2011). Any changes in future wind are determined from the IVRs between wind and the other climate variables. Wind was not changed by any CFs for the Caribbean.

Appendix 3: Calculation of Change Factors and their application

For a baseline climate, the parameters within the WG are fitted using daily measurements of the weather from a meteorological station in the Caribbean. This allows stochastic simulation of the present day climate. In order to simulate for future scenarios, model parameters are altered through the application of Change Factors (CFs) derived from RCM simulations available for the region with a 25km resolution (see Section 2.4, *Available Climate Model Projections*). The calculation of each of these CFs from RCM simulations is detailed here.

In summary, the rainfall statistics and standardisation parameters of secondary and tertiary variables are altered according to the change (proportional or difference) between the same property calculated from the 30-year future and the 30-year control simulations of an RCM. Here the control period is chosen to be 1971-2000 or 1981-2010 with three futures: the 2020s (2011-40), 2050s (2041-2070) and the 2080s (2071-2100).

A3.1 Change Factors for Precipitation Data

First, daily precipitation accumulations less than 1mm from an RCM grid box are set to zero. Five precipitation statistics are then estimated for the adjusted time series for each calendar month:

P_Mean, Mean daily rainfall (mm);

P_Var, sample variance of daily rainfall (mm^2);

PDRY, proportion of days with < 1.0 mm rainfall;

P_Skew, skewness coefficient of daily rainfall

i.e. $\sum_{i=1}^{n}\left(P_i - P_Mean\right)^3 \Big/ (n-1)P_var^{3/2}$, a non-dimensional quantity, (e.g. Metcalfe, 1994, p56);

and *P_AC*, is the daily lag-one autocorrelation. These five statistics are calculated for each calendar month for both the climate model's control, Ctrl, and future, fut, scenarios.

Following Burton et al. (2010) the CF for mean daily rainfall is calculated as a ratio, α_{P_Mean} = P_Mean_{fut} / P_Mean_{Ctrl} , for each calendar month. The CFs for *P_Var* and *P_Skew* are similarly calculated as ratios. However, when calculating the monthly CFs for *PDRY* a

transform is first applied to the control and future scenario estimates, $tPD = PDRY/(1-PDRY)$, before the ratio is calculated as usual, i.e. $\alpha_{PD} = tPD_{fut} / tPD_{Ctrl}$. The CF for *P_AC* is similarly calculated as the ratio of the transformed RCM estimates using the transform

$tAC = (1+P_AC)/(1-P_AC)$.

A3.2 Change Factors for Secondary and Tertiary variables

Similarly as for the precipitation statistics, estimates of the standardisation properties of each of the secondary and tertiary variables are determined from the 30-year RCM scenario for a specific 25km grid box. These include mean values of *T*, *R*, *S* and *VP* for each month (and transition where necessary), where *T* and *R* are calculated from *Tx* and *Tn* as usual and *VP* is calculated from the daily Relative Humidity variable by estimating the Saturation Vapour Pressure appropriate for the given *T*. Additionally, variances of *T* and *R* are calculated. As for precipitation these six statistics are calculated for each calendar month for both the climate model's control, Ctrl, and future, fut, scenarios.

In contrast to the CF for mean precipitation, the CF for *T* is calculated as a *difference*, i.e. $\alpha_T = T_{fut} - T_{Ctrl}$. Similarly, the CFs for *R*, *S* and *VP* are also calculated as differences. However, the CFs for the variance of both *T* and *R* are calculated as ratios. The CFs for primary, secondary and tertiary variables are summarized in Table 1.

A3.3 Application of Change Factors to parameterize the WG for future climate scenarios

To estimate the properties of rainfall in the downscaled future scenario (dfs), CFs are applied to the four observed meteorological properties used here in the rainfall model parameterization to represent the observed baseline climate (see §3.3). For the three ratio-type CFs (see Table 1), the future scenario estimate is calculated, e.g. for the mean, as $P_Mean_{dfs} = \alpha_{P_Mean}$ x $P_Mean_{baseline}$. For the two transformed variables, the baseline estimate is first transformed as for each RCM estimate, then the CF applied to determine a transformed downscaled future scenario estimate, e.g. tAC_{dfs} . Finally the estimate may be obtained using the appropriate back-transformation, i.e. $PDRY_{dfs} = tPDRY_{dfs}/(1+tPDRY_{dfs})$ or $P_AC_{dfs} = (tAC_{dfs}-1)/(tAC_{dfs}+1)$. Once the five monthly properties of the downscaled future

scenario are estimated, the rainfall model is fitted to this scenario as usual, as described in Appendix A2.1.

For the secondary and tertiary variables, the CFs are applied directly to the parameters used to describe the standardisation of the conditioned autoregressive model on a monthly basis. Thus the two temperature related ratio type CFs (see Table 1) are multiplied by the fitted baseline variance statistics to calculate the equivalent downscaled future scenario standardisation statistics, as for the P_Mean statistic. The difference type change factors (see Table 1) for *T*, *R*, *VP* and *S* are applied by adding each CF to the standardisation-mean parameter, to estimate that parameter's value for the downscaled future scenario. There is a correction step described in Jones et al. (2011) which is also applied to *T* and also to *R*, to ensure that the correct change factor is prescribed. This accounts for changes in *T* (and then subsequently in *R*) that occur as a result of changes in Precipitation. If, for example, less precipitation is projected in the future, it will likely become warmer. This aspect is accounted for so the projected changes will average to the CFs given for the non-precipitation variables by the RCM simulation. These types of correction factors are referred to second-order adjustments by Wilks (2012). Even though the issue was recognized earlier by Katz (1996) it does not appear to be applied for most WGs with CFs.

As stated in the main text, the numerous inter-variable relationships are not considered well reproduced by the RCMs and so are assumed to remain unchanged in the future. Thus the standard deviations of the tertiary variables and the coefficients of the IVRs (*a*, *b*, *c*, *d*, *e*, *f* and *g*) remain unchanged for the future scenario. Change factors are not used for wind. For similar work in the UK, the projections were not considered reliable (Jones et al., 2010, 2011).

Acknowledgements

The research presented in this paper was carried out as part of the CARIWIG project which was funded by the Climate Development Knowledge Network (CDKN). The observed Meteorological datasets were made available by Cuban Instituto de Meteorologia (INSMET), the Caribbean Institute of Meteorology and Hydrology (CIMH, http://www.cimh.edu.bb/), the Belize National Meteorological Service (http://www.hydromet.gov.bz/), the Jamaican Meteorological Service and the Antigua and Barbuda Meteorological Service. These

institutes should be contacted directly for access to the station data. The climate model data used in this study was produced by the Caribbean Climate Modelling Group. These datasets may be obtained either through the INSMET website (http://www.met.inf.cu/asp/genesis.asp?TB0=PLANTILLAS&TB1=INICIAL) or through the CARIWIG web site (http://www.cariwig.org/).

This document is an output from a project funded by the UK Department for International Development (DFID) and the Netherlands Directorate-General for International Cooperation (DGIS) for the benefit of developing countries. However, the views expressed and information contained in it are not necessarily those of or endorsed by DFID, DGIS or the entities managing the delivery of the CDKN, which can accept no responsibility or liability for such views, completeness or accuracy of the information or for any reliance placed on them.

References

Bautista F, Bautista D, Delagdo-Carranza C, 2009: Calibration of the equations of Hargreaves and Thornthwaite to estimate potential evapotranspiration in semi-arid and subhumid tropical climate for regional applications. *Atmósfera* **22**, 331-348.

Burton A, Kilsby CG, Fowler HJ, Cowpertwait PSP, O'Connell PE, 2008: RainSim: A spatial-temporal stochastic rainfall modelling system. *Environmental Modelling & Software*, **23**(12), 1356-1369.

Burton A, Fowler HJ, Blenkinsop S, Kilsby CG, 2010: Downscaling transient climate change using a Neyman–Scott Rectangular Pulses stochastic rainfall model. *Journal of Hydrology* 2010, **381**(1-2), 18-32.

Campbell JD, Taylor MA, Stephenson TS, Watson RA, Whyte FS, 2010: Future climate of the Caribbean from a regional climate model. *Int. J. Clim.*, **31**, 1866-1878, doi: 10.1002/joc.2200

Centella A, Bezanilla A, Leslie K, 2007: Assessing the uncertainty of Climate Change in the Caribbean using the PRECIS outputs. Technical Report, Community Caribbean Climate Change Center, Belmopan, Belize.

Centella-Artola A, Taylor MA, Bezanilla-Morlot A, Martinez-Castro D, Campbell JD, Stephenson TS, Vichot A, 2015: Assessing the effect of domain size over the Caribbean Region using the PRECIS Regional Climate Model. *Climate Dynamics* **44**, 1901-1918 (available online at DOI 10.1007/s00382-014-2272-8).

Chen J, Brissette FP, Leconte R, 2012: Downscaling of weather generator parameters to quantify hydrological impacts of climate change. *Climate Research* **51**, 185-200.

Christensen JH, Hewitson B, Busuioc A, Chen A, Gao X, Held I, Jones R, Kolli RK, Kwon W-T, Laprise R, Magaña Rueda V, Mearns L, Menéndez CG, Räisänen J, Rinke A, Sarr A, Whetton P, 2007: Regional Climate Projections. In: Climate Change 2007: The Physical Science Basis. Contribution of Working Group I to the Fourth Assessment Report of the Intergovernmental Panel on Climate Change [Solomon, S., Qin, D., Manning, M., Chen, Z., Marquis, M., Averyt, K.B., Tignor M. and Miller H.L. (eds.)]. Cambridge University Press, Cambridge, United Kingdom and New York, NY, USA.

Christensen JH, Krishna Kumar K, Aldrian E, An S-I, Cavalcanti IFA, de Castro M, Dong W, Goswami P, Hall A, Kanyanga JK, Kitoh A, Kossin J, Lau N-C, Renwick J, Stephenson DB, Xie S-P, Zhou T, 2013: Climate Phenomena and their Relevance for Future Regional Climate Change. In: Climate Change 2013: The Physical Science Basis. Contribution of Working Group I to the Fifth Assessment Report of the Intergovernmental Panel on Climate Change [Stocker TF, Qin D, Plattner G-K, Tignor M, Allen SK, Boschung J, Nauels A, Xia Y, Bex V, Midgley PM (eds.)]. Cambridge University Press, Cambridge, United Kingdom and New York, NY, USA.

Cowpertwait PSP, O'Connell PE, Metcalfe AV, Mawdsley JA, 1996: Stochastic point process modelling of rainfall. 2. Regionalisation and disaggregation. *Journal of Hydrology*, **175**, 47–65.

Durban M, Glasby CA, 2001: Weather modelling using a multivariate latent Gaussian model. *Agricultural and Forest Meteorology*, **109**, 187–201.

Ekström M, Jones PD, Fowler H, Lenderink G, Buishand TA, Conway D, 2007: Regional climate model data used within the SWURVE project 1: projected changes in seasonal patterns and estimation of PET. *Hydrology and Earth Systems Science* **11**, 1069-1083.

Forsythe N, Fowler HJ, Blenkinsop S, Burton A, Kilsby CG, Archer DR, Harpham C, Hashmi MZ, 2014: Application of a stochastic weather generator to assess climate change impacts in a semi-arid climate: The Upper Indus Basin. *J Hydrology* **517**, 1019-1034.

Harris I, Jones PD, Osborn TJ, Lister DH, 2014: Updated high-resolution monthly grids of monthly climatic observations: the CRU TS 3.10 dataset. *Int. J. Climatol*., **34**, 623-642, DOI:10.1002/joc.3711.

Jenkins K, Hall J, Glenis V, Kilsby CG, McCarthy M, Goodess C, Smith D, Malleson N, Birkin M, 2014: Probabilistic spatial risk assessment of heat impacts and adaptations for London. *Climatic Change*, **124**(1-2), 105-117.

Jones PD, Kilsby CG, Harpham C, Glenis V, Burton A, 2010: UK Climate Projections science report: Projections of future daily climate for the UK from the Weather Generator, University of Newcastle, UK. Revised 2010. (http://ukclimateprojections.metoffice.gov.uk/22588).

Jones PD, Harpham C, Goodess CM, Kilsby CG, 2011: Perturbing a Weather Generator using change factors derived from Regional Climate Model simulations. *Nonlinear Processes in Geophysics* **18**, 503-511.

Jones PD, Harpham C, Harris I, Goodess CM, Burton A, Centella A, Taylor M, Bezanilla A, Campbell JD, Stephenson, TS, Joslyn O, Nicholls K, Baur T, 2015: Long-term trends in precipitation and temperature across the Caribbean. *Int. J. Climatol*. (re-submitted).

Karmalkar A, Taylor M, Campbell J, Stephenson T, New M, Centella A, Bezanilla A, Charlery J, 2013: A Review of Observed and Projected Changes in Climate for the Islands in the Caribbean. *Atmosfera*, **26**, 283-309.

Katz RW, 1996: Use of conditional stochastic models to generate climate change scenarios. *Climatic Change* **32**, 237–255.

Kilsby CG, Jones PD, Burton A, Ford AC, Fowler HJ, Harpham C, James P, Smith A, Wilby RL, 2007: A daily weather generator for use in climate change studies. *Environmental Modelling and Software* **22**, 1705-1719.

Knapp KR, Kruk MC, Levinson DH, Diamond HJ and Neumann CJ, 2010: The International Best Track Archive for Climate Stewardship (IBTrACS): Unifying tropical cyclone best track data. *Bull. Amer. Meteorol. Soc*., **91**, 363–376, DOI: 10.1175/2009BAMS2755.1.

Lu J, Sun G, McNulty SG, Amatya DM, 2005: A comparison of six potential evapotranspiration methods for regional use in the southeastern United States. *J. Amer. Water Resources Assoc. (JAWRA)* **39**, 621-633.

Maraun D, Wetterhall F, Ireson AM, Chandler RE, Kendon EJ, Widmann M, Brienen S, Rust HW, Sauter T, Themeßl M, Venema VKC, Chun KP, Goodess CM, Jones RG, Onof C, Vrac M, Thiele-Eich I, 2010: Precipitation downscaling under climate change: Recent developments to bridge the gap between dynamical models and the end user. *Reviews of Geophysics*, **48**, RG3003, doi:10.1029/2009RG000314.

Martynov A, Laprise R, Sushama L, Winger K, Šeparović L, Dugas B, 2013: Reanalysis-driven climate simulation over CORDEX North America domain using the Canadian Regional Climate Model, version 5: Model performance evaluation. *Clim. Dyn*. **41**, 2973-3005, http://link.springer.com/article/10.1007/s00382-013-1778-9.

Metcalfe AV, 1994: *Statistics in Engineering - A practical approach*, Chapman and Hall, 446pp.

Mitchell T, Carter, TR, Jones P, Hulme M, 2004: *A comprehensive set of high-resolution grids of monthly climate for Europe and the globe: the observed record (1901-2000) and 16 scenarios (2001-2100)* In *Tyndall Centre Working Paper 55*., 30pp.

Muneer T, 2004: *Solar Radiation and Daylight Models*, Elsevier Butterworth-Heineman.

New M, Hulme M, Jones, PD, 1999: Representing twentieth-century space-time climate variability. Part I: Development of a 1961-90 mean monthly terrestrial climatology. *J. Climate* **12**, 829-856.

Nicks AD, Lane LJ, Gander GA, 1995: Chapter 2: weather generator. In: Flanagan DC, Nearing MA (eds) *USDA–Water Erosion Prediction Project: Hillslope profile and watershed model documentation*. NSERL Report No. 10, West Lafayette, IN.

Onof C, Chandler RE, Kakou A, Northrop P, Wheater HS, Isham V, 2000: Rainfall modelling using Poisson-cluster processes: a review of developments. *Stochastic Environmental Research and Risk Assessment*, **14**, 384–411.

Parry ML, Canziani OF, Palutikof JP, van der Linden PJ, Hanson CE (eds), 2007: Contribution of Working Group II to the Fourth Assessment Report of the Intergovernmental Panel on Climate Change, 2007 Cambridge University Press, Cambridge, United Kingdom and New York, NY, USA, 976pp.

Perreira AP, Paes de Camargo A, 1989: An analysis of the criticism of Thornthwaite's equation for estimating potential evapotranspiration. *Agricultural and Forest Meteorology* **46**, 149-157.

Prudhomme C, Reynard N, Crooks S., 2002: Downscaling of global climate models for flood frequency analysis: where are we now? Hydrological Processes 16, 1137–1150.

Racsko P, Szeidl L, Semenov M, 1991: A Serial Approach to Local Stochastic Weather Models, *Ecological Modelling* **57**, 27–41.

Richardson CW, 1981: Stochastic simulation of daily precipitation, temperature, and solar radiation. *Water Resources Res*. **17**, 182−190

Richardson C, Wright DA, 1984: WGEN: a model for generating daily weather variables. U.S. Dept. Agr., Agricultural Research Service, Publ. ARS-8, p. 38.

Robock A, Turco RP, Harwell MA, Ackerman TE, Andressen R, Chang H-S, Sivakumar MVK, 1993: Use of General Circulation Model Output in the Creation of Climate Change Scenarios for Impact Analysis, *Climatic Change* **23**, 293-335.

Schmidli J, Goodess CM, Frei C, Haylock MR, Hundecha Y, Ribalaygua J, Schmith T, 2007: Statistical and dynamical downscaling of precipitation: An evaluation and comparison of scenarios for the European Alps. *Journal of Geophysical Research*, **112**, D04105, doi: 10.1029/2005JD007026.

Semenov MA, 2008: Simulation of extreme weather events by a stochastic weather generator, *Climate Research*, **35**, 203-212.

Semenov MA, Barrow EM, 1997: Use of a stochastic weather generator in the development of climate change scenarios. *Climatic Change* **35**, 397–414.

Stephenson TS, Van Meerbeeck CJ, Vincent LA, Allen T, McLean N, Peterson TC Taylor MA, Aaron-Morrison AP, Auguste T, Bernard D, Boekhoudt JRI, Blenman RC, Braithwaite GC, Brown G, Butler M, Cumberbatch CJM, Kirton-Reed L, Etienne-Leblanc S, Lake DE, Martin DE, McDonald JL, Zaruela MO, Porter AO, Ramirez MS, Stoute S, Tamar GA, Trotman AR, Roberts BA, Mitro SS, Shaw A, Spence JM, Winter A., 2014: Changes in Extreme Temperature and Precipitation in the Caribbean Region, 1961-2010. *Int. J. Climatol*, **34**, 2957-2971, DOI: 10.1002/joc.3889.

Taylor MA, Alfaro EJ, 2005: Central America and the Caribbean, Climate of. In *Encyclopedia of World Climatology* (Ed. J. E. Oliver). Springer, Berlin, pp183-188.

Taylor MA, Centella J, Chalery I, Forrajero A, Bezanilla A, Campbell R, Rivero T, Stephenson T, Whyte E, Watson R, 2007: Glimpses of the future. A briefing from the PRECIS Caribbean Climate Change Project, Caribbean Community Climate Change Center, Belmopan, Belize 24pp.

Thornthwaite CW, 1948: An approach toward a rational classification of climate. *Geographical Review* **38**, 55-94.

Velghe T, Troch PA, De Troch FP, Van de Velde J, 1994: Evaluation of cluster-based rectangular pulses point process models for rainfall. *Water Resources Research*, **30**, 2847–2857.

Wilby RL, Conway D, Jones PD, 2002: Prospects for downscaling seasonal precipitation variability using conditioned weather generator parameters. *Hydrological Processes* **16**, 1215-1234.

Wilks DS, 1992: Adapting stochastic weather generation algorithms for climate change studies. *Climatic Change* **22**, 67–84.

Wilks DS, 1999: Multisite downscaling of daily precipitation with a stochastic weather generator. *Climate Research* **11**, 125–136.

Wilks DS, 2010: Use of stochastic weather generators for precipitation downscaling. *WIREs, Climate Change*, **1**, 898-907, DOI: 10.1002/wcc.85.

Wilks DS, 2012: Stochastic weather generators for climate-change downscaling, part II: multivariable and spatially coherent multisite downscaling. *WIREs Climate Change* **3**, 267-278.

Wilks DS, Wilby RL, 1999: The weather generation game: a review of stochastic weather models. *Progress in Physical Geography*, **23**, 329–357.

Wong G, Maraun D, Vrac M, Widmann M, Eden JM Kent T, 2014: Stochastic model output statistics for bias correcting and downscaling precipitation including extremes *J. Climate* 27,6940-6959.

Xu C-Y, Singh VP, 2001: Evaluation and generalization of temperature-based methods for calculating evaporation. *Hydrological Processes* **15**, 305-319.

Zhang XC, 2005: Spatial downscaling of global climate model output for site-specific assessment of crop production and soil erosion. *Agricultural and Forest Meteorology* **135**, 215−229.

Zhang X, Alexander L, Hegerl GC, Jones PD, Klein Tank A, Peterson TC, Trewin B, Zwiers FW, 2011: Indices for monitoring changes in extremes based on daily temperature and precipitation data*. WIREs Climate Change*, **2**, 851-870, doi:10.1002/wcc/147.

Tables

Table 1: Summary of daily weather variables related to the WG and their perturbation for future climate scenarios. The full set of six generated WG variables is provided with *primary*, *secondary* and *tertiary* labels indicating the order in which sets of variables are calculated, each dependant on the previous sets. Subsequently, a further set of *calculated* variables may be estimated using empirical relationships external to the structure of the WG. A list of change factors and their type, as used to characterise the RCM projections of future climate change, are provided and associated with each set of variables.

Variable	**Change factors and sequence of application**
Primary generated variable: Precipitation, *P*, (mm)	Mean wet day amount (ratio) Precipitation daily variance (ratio) Precipitation probability dry (transform) Precipitation skewness (ratio) Precipitation lag-1 autocorrelation (transform)
Secondary generated variables: Minimum temperature, *Tn*, (degrees C) Maximum temperature, *Tx*, (degrees C)	Temperature diurnal mean (difference)* Variance of diurnal mean temperature (ratio)* Diurnal temperature range (difference)* Variance of diurnal temperature range (ratio)*
Tertiary generated variables: Vapour pressure, *VP*, (hPa) Sunshine duration, *S*, (hours) Wind speed, *W*, (ms^{-1})	Vapour pressure daily average (difference) Sunshine daily average (difference)
Calculated variables: Relative humidity, *RH*, (%) Diffuse radiation ($kWhm^{-2}$) (Muneer, 2004) Direct radiation ($kWhm^{-2}$) (Muneer, 2004) Reference potential evapotranspiration (mm) (Ekström et al., 2007)	

*Adjusted for changes earlier in the perturbation sequence

Table 2: The five ETCCDI indices of extremes used, the acronyms are as defined by ETCCDI.

Description of indices	Formal Definition
Daily precipitation amount during intense events (R95p)	Precipitation amount exceeded only 5% of the time
Maximum 5-day precipitation (RX5day)	Maximum 5-day precipitation total
Maximum number of consecutive dry days (CDD)	Maximum number of consecutive dry days
Number of “Hot days” (TX90p)	% of days when maximum temperature is greater than the 90th percentile value
Number of “Warm nights” (TN90p)	% of days when minimum temperature is greater than the 90th percentile value

Figure Captions

Figure 1: Locations of the 42 sites across the Caribbean with sufficient available daily data for WG calibration. The stations are listed within Appendix 1.

Figure 2: Comparison of PET calculations (for Philip Goldson International Airport in Belize) for the observed data (green - O) with the same data, but with vapour pressure replaced by the calculation from Tn (yellow - N). The boxplots are standard, with the notch being plotted at the median value (50th percentile) and the upper and lower end of the box at the 75th and 25th percentiles. The whiskers are plotted up to 1.5 times the Interquartile Range (IQR) below and above the 25th and 75th percentiles. Values outside the whiskers are plotted as circles.

Figure 3: As Figure 1, but for the Melville Hall site on Dominica.

Figure 4a: Observational average (blue, shown as a plus sign), WG range for the control period (1981-2010 as black dots and error bars) and WG-based projections for the 2020s (2011-40) as red dots and error bars) for each month for the RCM grid cell that encloses Husbands, Barbados for precipitation and temperature variables. The simulated values are the means of 100 30-year weather generator runs. The lines and bars show the variability of the 100 runs (plotted as plus/minus two standard deviations around the mean). Other climate variables are shown in Figure 6b. The driving GCM here was HadCM3Q0 forcing the PRECIS RCM.

Figure 4b: Observational average (blue, shown as a plus sign), WG range for the control period (1981-2010 as black dots and error bars) and WG-based projections for the 2020s (2011-40 as red dots and error bars) for each month for the RCM grid cell that encloses Husbands, Barbados for the other climate variables. The simulated values are the means of 100 30-year weather generator runs. The lines and bars show the variability of the 100 runs (plotted as plus/minus two standard deviations around the mean). Precipitation and Temperature variables are shown in Figure 6a. The driving GCM here was HadCM3Q0 forcing the PRECIS RCM.

Figure 5a: Observational average (blue, shown as a plus sign), WG range for the control period (1981-2010 as black dots and error bars) and WG-based projections for the 2050s (2041-2070 as red dots and error bars) for each month for the RCM grid cell that encloses Philip Goldson Airport, Belize for precipitation and temperature variables. The simulated values are the means of 100 30-year weather generator runs. The lines and bars show the variability of the 100 runs (plotted as plus/minus two standard deviations around the mean). Other climate variables are shown in Figure 7b. The driving GCM here was ECHAM5 forcing the PRECIS RCM.

Figure 5b: Observational average (blue, shown as a plus sign), WG range for the control period (1981-2010 as black dots and error bars) and WG-based projections for the 2050s (2041-70 as red dots and error bars) for each month for the RCM grid cell that encloses Philip Goldson Airport, Barbados for the other climate variables. The simulated values are the means of 100 30-year weather generator runs. The lines and bars show the variability of the 100 runs (plotted as

plus/minus two standard deviations around the mean). Precipitation and Temperature variables are shown in Figure 7a. The driving GCM here was ECHAM5 forcing the PRECIS RCM.

Figure 6: Format as Figures 4a and 4b for the Husbands site in Barbados, but showing the frequency of the number of days each month with daily precipitation amounts exceeding 50, 80 and 150mm. The driving GCM here was HadCM3Q0 forcing the PRECIS RCM. The frequency count is the total over the 30-year period.

Figure 7: Format as Figures 5a and 5b for Philip Goldson Airport in Belize, but showing the frequency of the number of days each month with daily precipitation amounts exceeding 50, 80 and 150mm. The driving GCM here was ECHAM5 forcing the PRECIS RCM. The frequency count is the total over the 30-year period.

Figure 8: Format as Figures 6 and 7 for Husbands, Barbados for 2020s, but extremes calculated from the ETCCDI CLIMDEX software. Three extremes are calculated monthly (the number of days and nights above the 90th percentile of Tx and Tn respectively and the maximum 5-day rainfall total in each month) and two annually (the number of consecutive dry days and the rainfall amount exceeded only 5% of the time). The driving GCM here was HadCM3Q0Q0 forcing the PRECIS RCM.

Figure 9: Format as Figures 6 and 7 for Philip Goldson Airport, Belize for the 2050s, but extremes calculated from the ETCCDI CLIMDEX software. Three extremes are calculated monthly (the number of days and nights above the 90th percentile of Tx and Tn respectively and the maximum 5-day rainfall total in each month) and two annually (the number of consecutive dry days and the rainfall amount exceeded only 5% of the time). The driving GCM here was ECHAM5 forcing the PRECIS RCM.

Figures

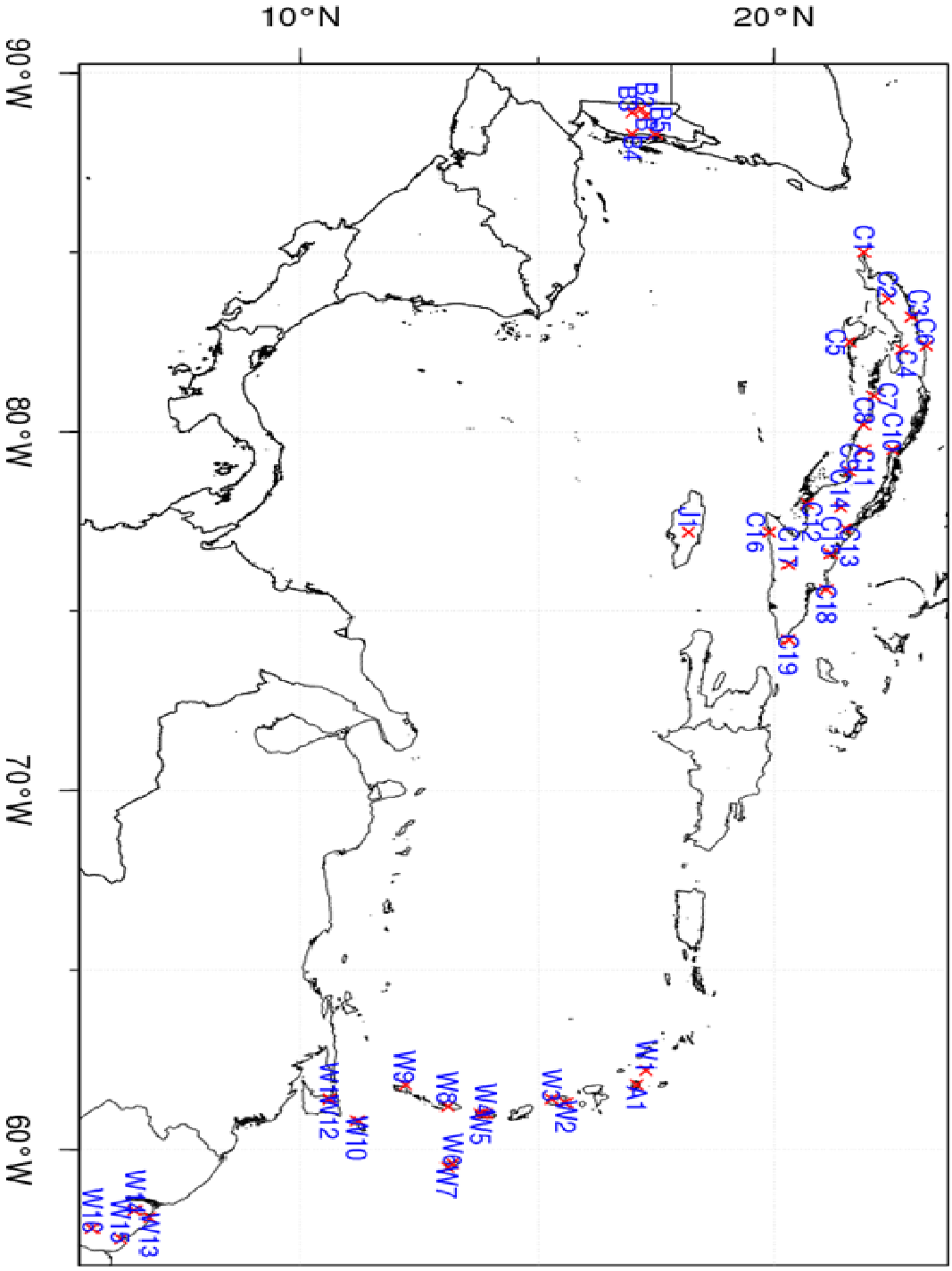

Figure 1: Locations of the 42 sites across the Caribbean with sufficient available daily data for WG calibration. The stations are listed within Appendix 1.

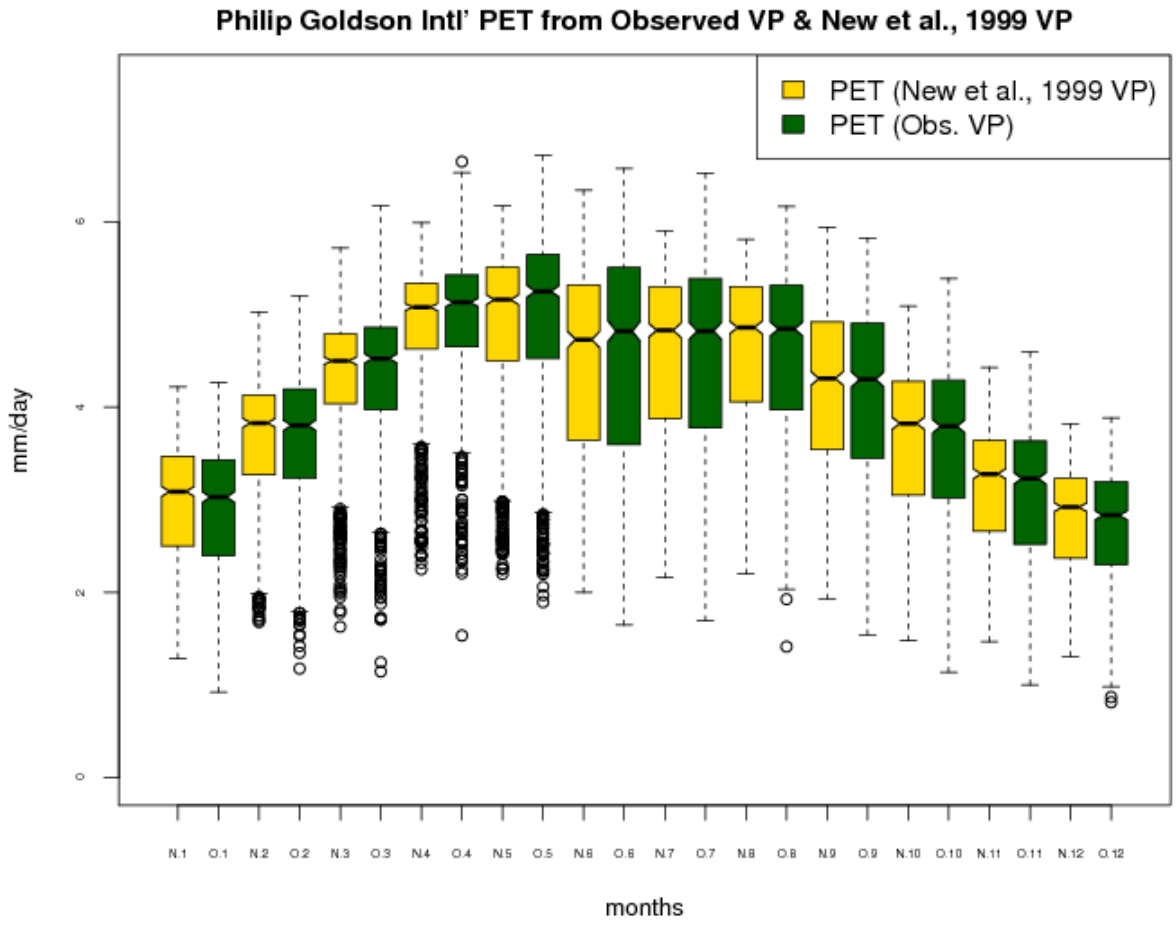

Figure 2: Comparison of PET calculations (for Philip Goldson International Airport in Belize) for the observed data (green - O) with the same data, but with vapour pressure replaced by the calculation from Tn (yellow – N). The boxplots are standard, with the notch being plotted at the median value (50th percentile) and the upper and lower end of the box at the 75th and 25th percentiles. The whiskers are plotted up to 1.5 times Interquartile Range (IQR) below and above the 25th and 75th percentiles. Values outside the whiskers are plotted as circles.

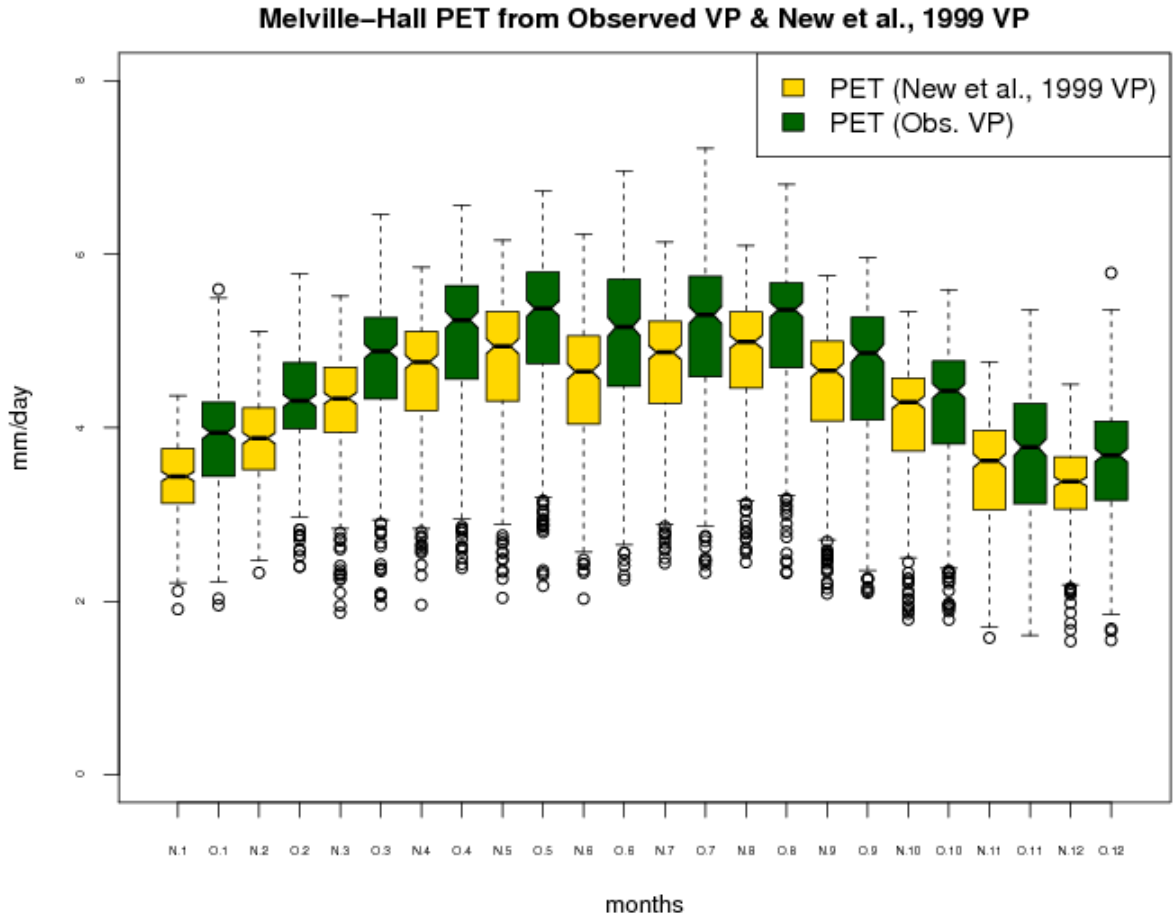

Figure 3: As Figure 2, but for the Melville Hall site on Dominica.

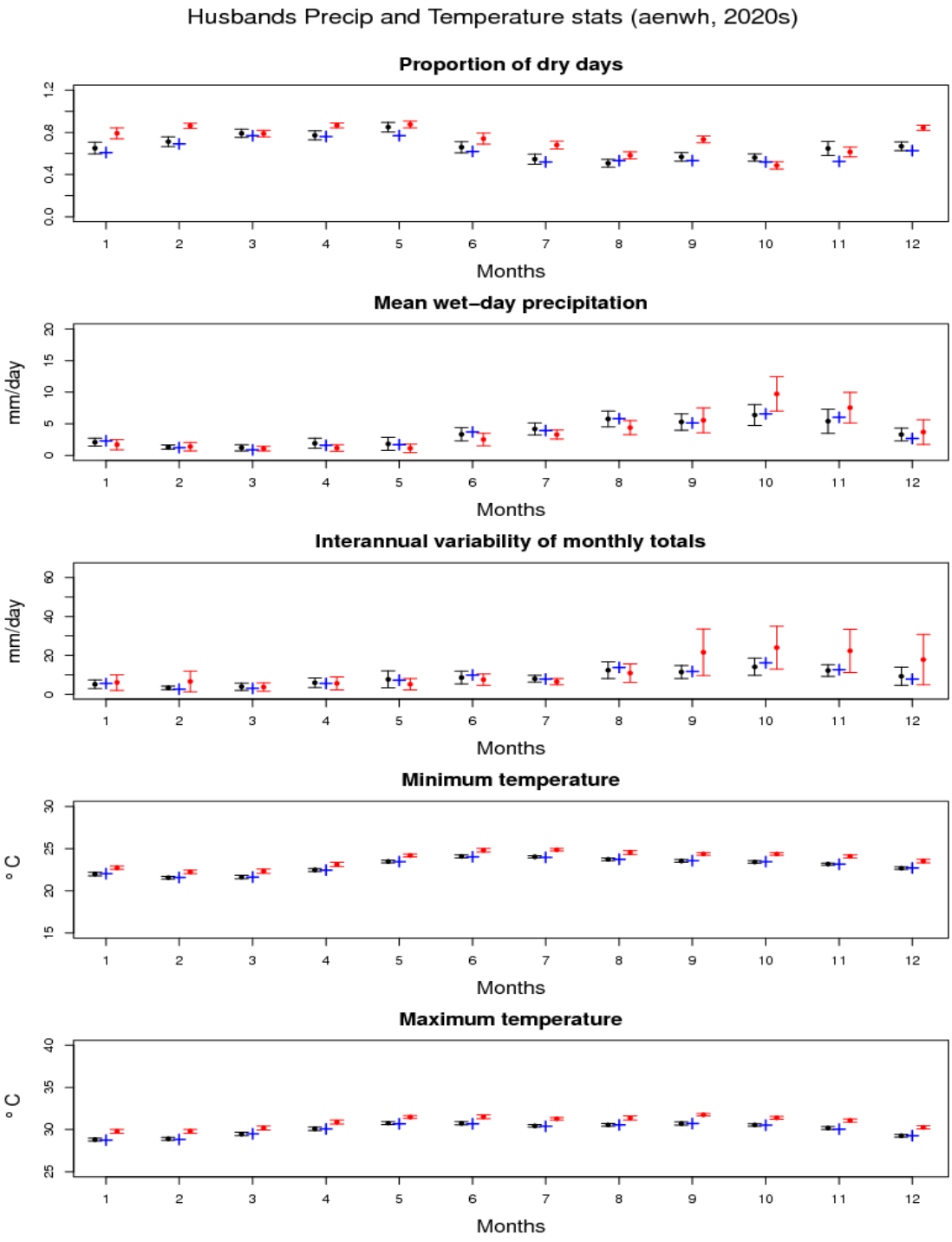

Figure 4a: Observational average (blue, shown as a plus sign), WG range for the control period (1981-2010 as black dots and error bars) and WG-based projections for the 2020s (2011-2040 as red dots and error bars) for each month for the RCM grid cell that encloses Husbands, Barbados for precipitation and temperature variables. The simulated values are the means of 100 30-year weather generator runs. The lines and bars show the variability of the 100 runs (plotted as plus/minus two standard deviations around the mean). Other climate variables are shown in Figure 6b. The driving GCM here was HadCM3Q0 forcing the PRECIS RCM.

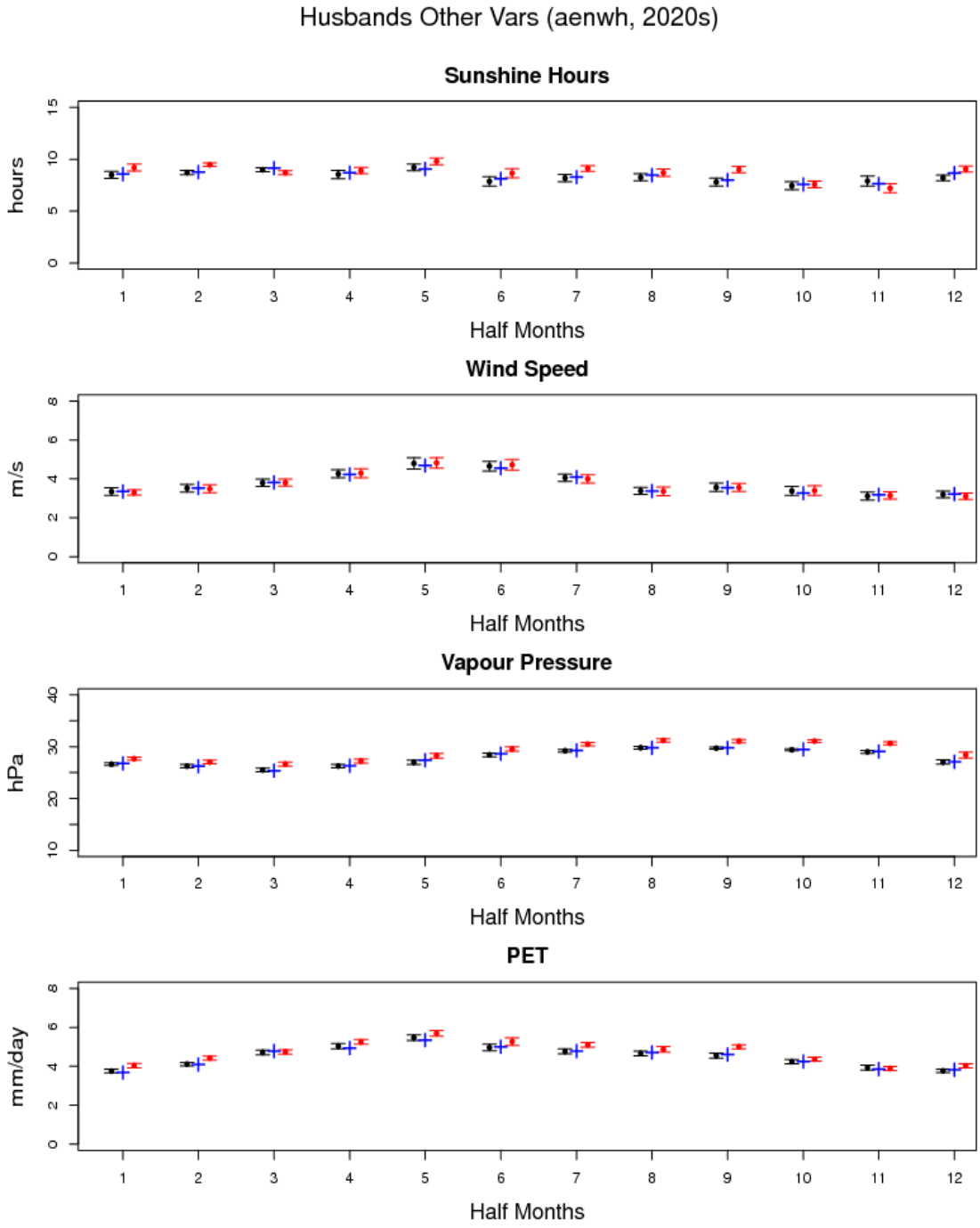

Figure 4b: Observational average (blue, shown as a plus sign), WG range for the control period (1981-2010 as black dots and error bars) and WG-based projections for the 2020s (2011-2040 as red dots and error bars) for each month for the RCM grid cell that encloses Husbands, Barbados for the other climate variables. The simulated values are the means of 100 30-year weather generator runs. The lines and bars show the variability of the 100 runs (plotted as plus/minus two standard deviations around the mean). Precipitation and Temperature variables are shown in Figure 6a. The driving GCM here was HadCM3Q0 forcing the PRECIS RCM.

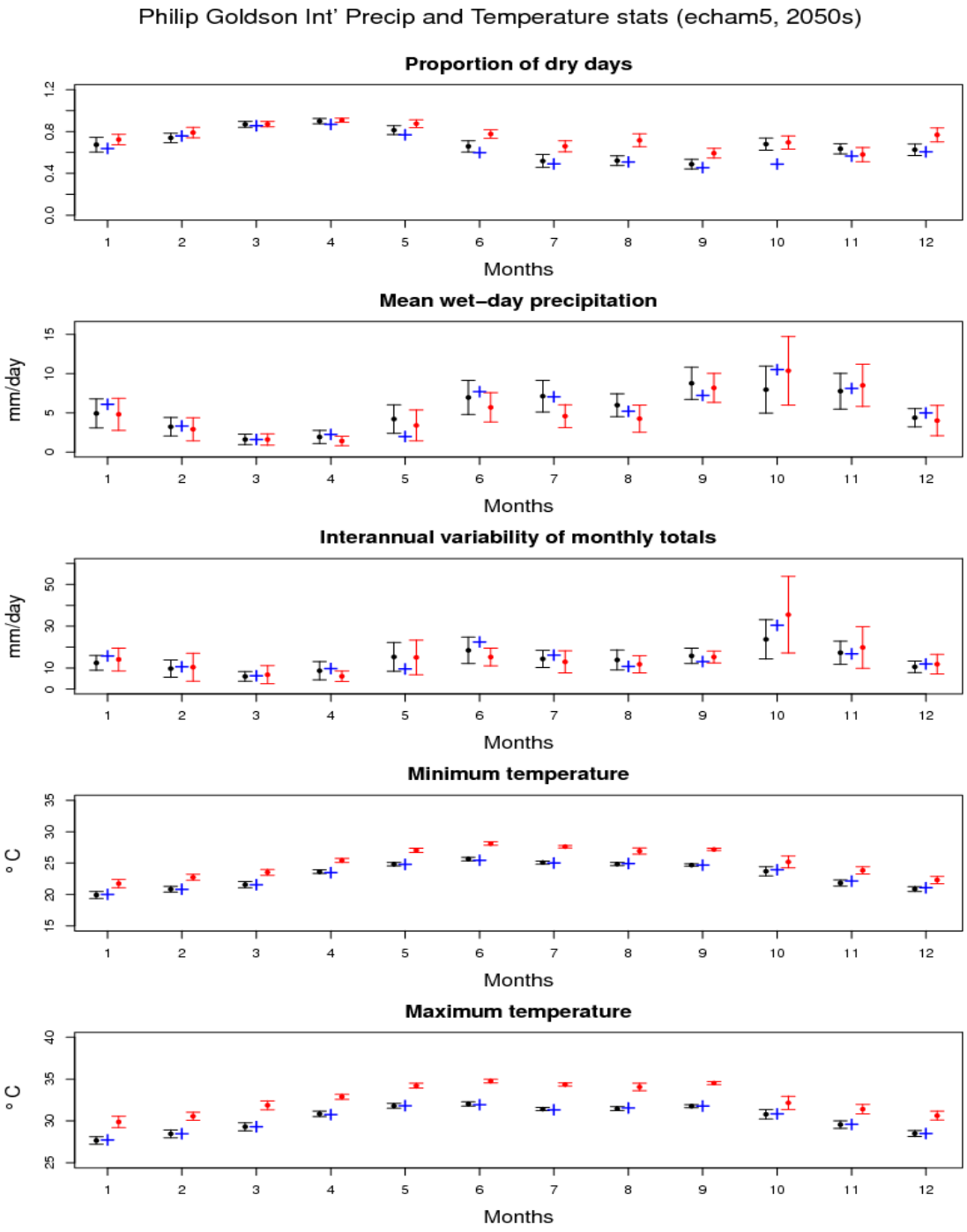

Figure 5a: Observational average (blue, shown as a plus sign), WG range for the control period (1981-2010 as black dots and error bars) and WG-based projections for the 2050s (2041-2070 as red dots and error bars) for each month for the RCM grid cell that encloses Philip Goldson Airport, Belize for precipitation and temperature variables. The simulated values are the means of 100 30-year weather generator runs. The lines and bars show the variability of the 100 runs (plotted as plus/minus two standard deviations around the mean). Other climate variables are shown in Figure 7b. The driving GCM here was ECHAM5 forcing the PRECIS RCM.

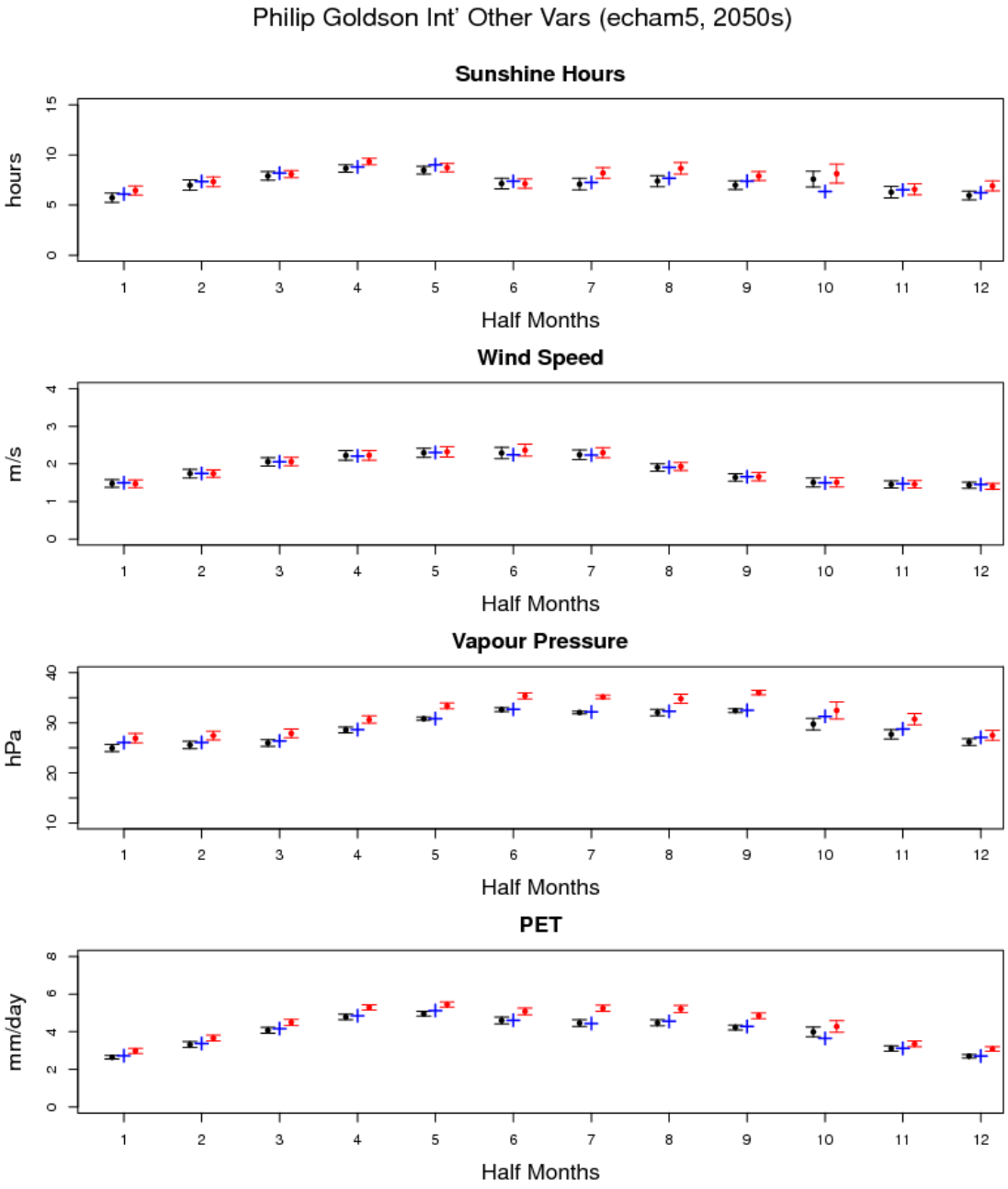

Figure 5b: Observational average (blue, shown as a plus sign), WG range for the control period (1981-2010 as black dots and error bars) and WG-based projections for the 2050s (2041-2070 as red dots and error bars) for each month for the RCM grid cell that encloses Philip Goldson Airport, Barbados for the other climate variables. The simulated values are the means of 100 30-year weather generator runs. The lines and bars show the variability of the 100 runs (plotted as plus/minus two standard deviations around the mean). Precipitation and Temperature variables are shown in Figure 7a. The driving GCM here was ECHAM5 forcing the PRECIS RCM.

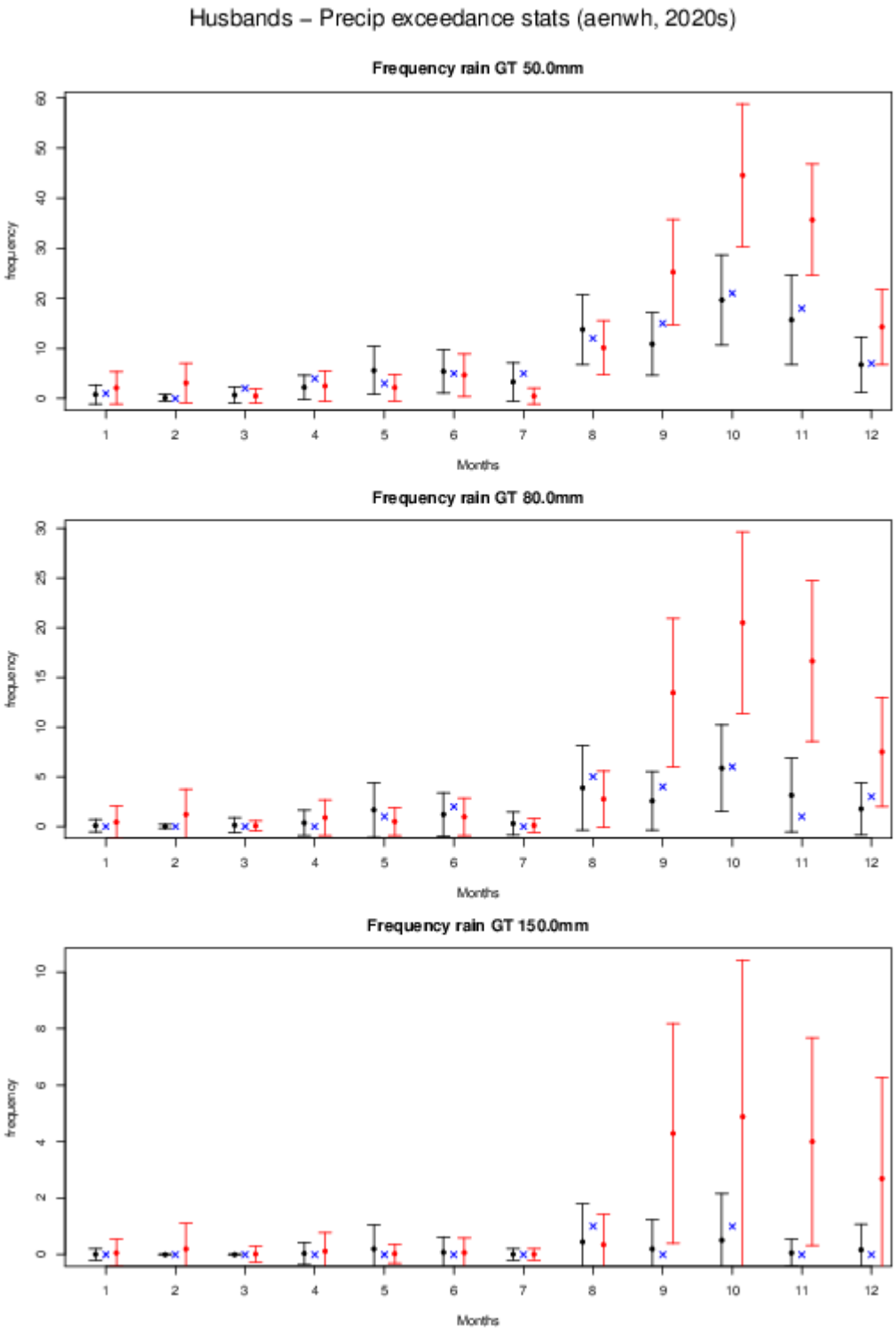

Figure 6: Format as Figures 4a and 4b for the Husbands site in Barbados, but showing the frequency of the number of days each month with daily precipitation amounts exceeding 50, 80 and 150mm. The driving GCM here was HadCM3Q0 forcing the PRECIS RCM. The count is the total over the 30-year period.

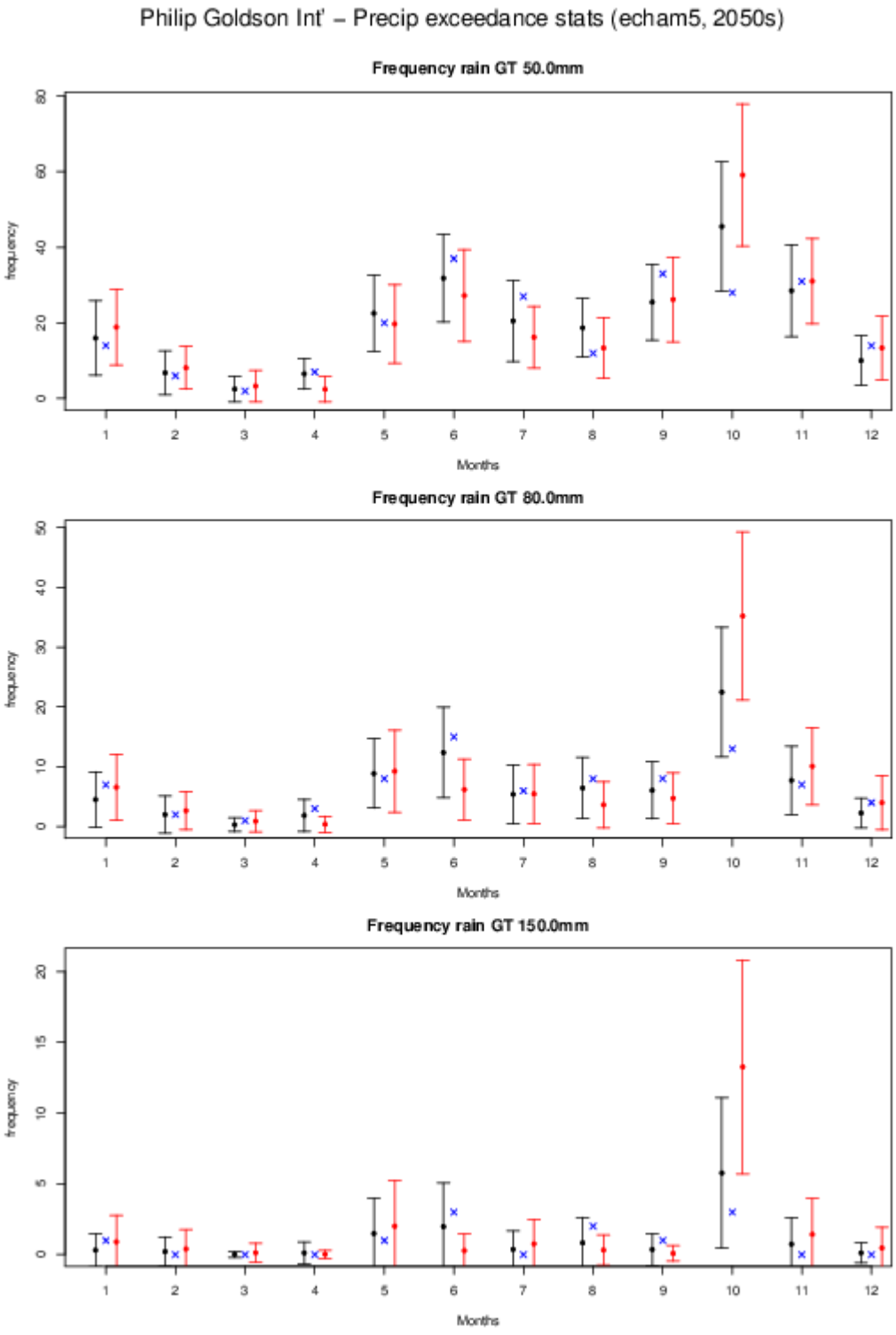

Figure 7: Format as Figures 5a and 5b for Philip Goldson Airport in Belize, but showing the frequency of the number of days each month with daily precipitation amounts exceeding 50, 80 and 150mm. The driving GCM here was ECHAM5 forcing the PRECIS RCM. The frequency count is the total over the 30-year period.

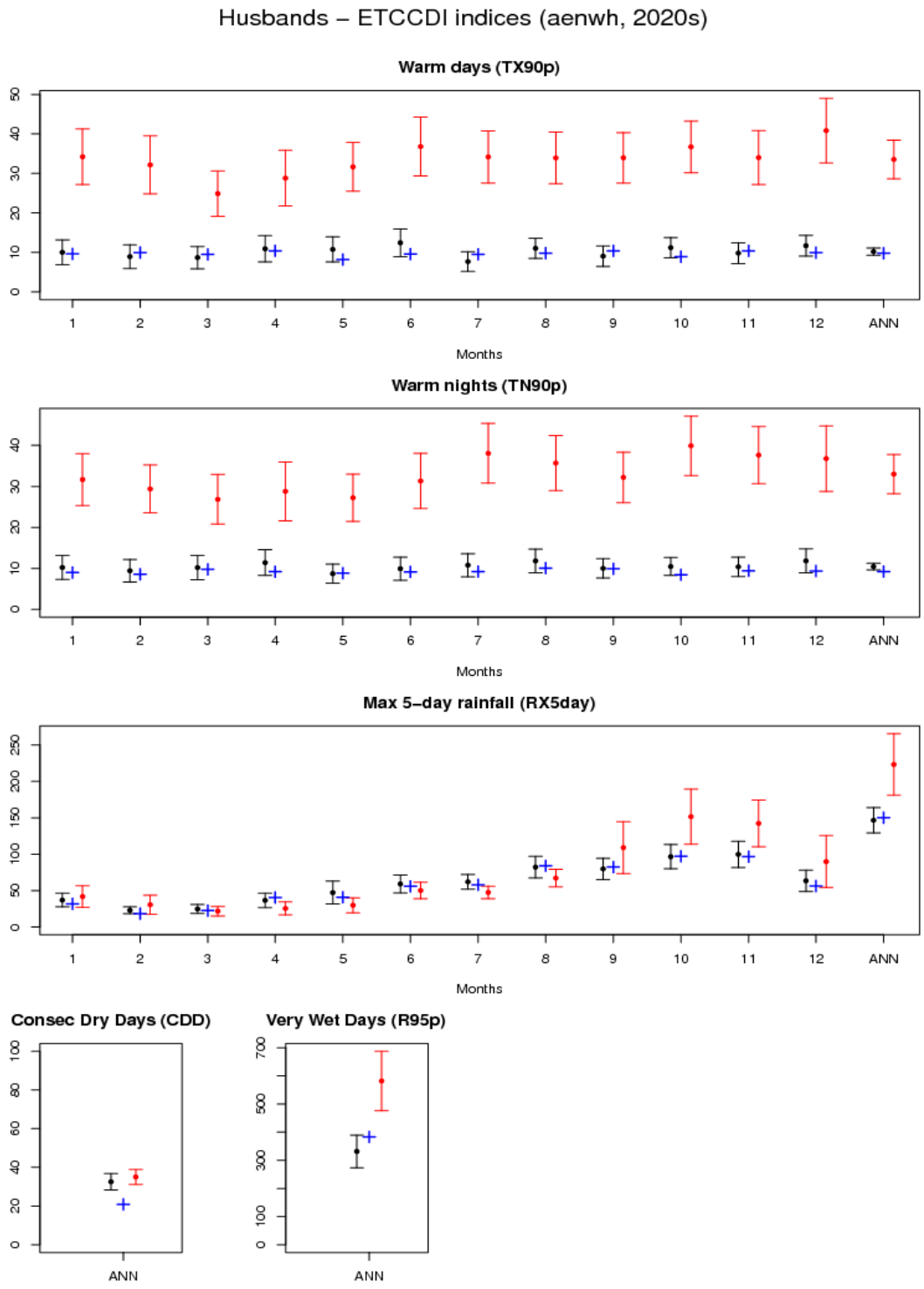

Figure 8: Format as Figures 6 and 7 for Husbands, Barbados for 2020s, but extremes calculated from the ETCCDI CLIMDEX software. Three extremes are calculated monthly (the number of days and nights above the 90th percentile of Tx and Tn respectively and the maximum 5-day rainfall total in each month) and two annually (the number of consecutive dry days and the rainfall amount exceeded only 5% of the time). The driving GCM here was HadCM3Q0Q0 forcing the PRECIS RCM.

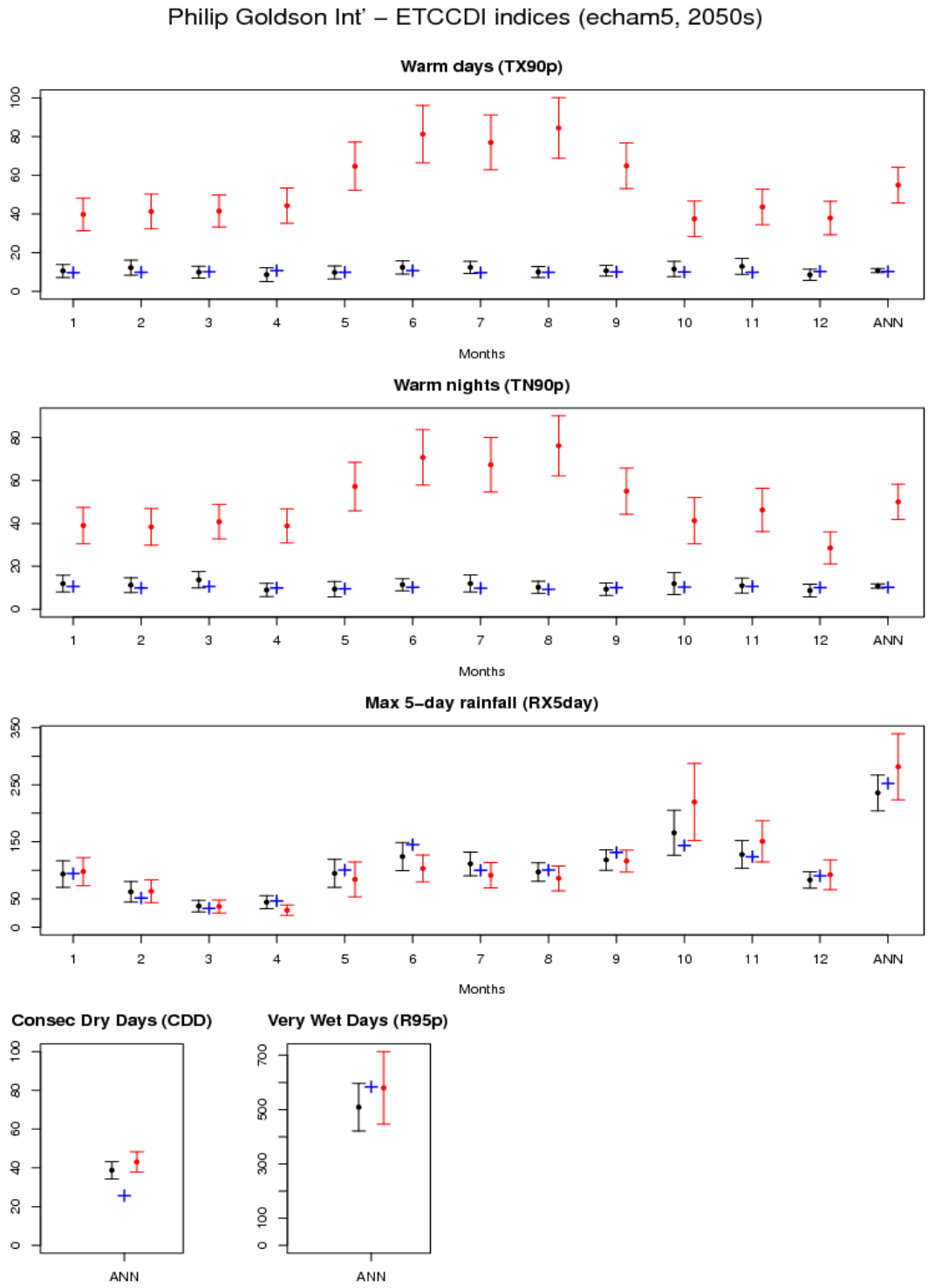

Figure 9: Format as Figures 6 and 7 for Philip Goldson Airport, Belize for the 2050s, but extremes calculated from the ETCCDI CLIMDEX software. Three extremes are calculated monthly (the number of days and nights above the 90th percentile of Tx and Tn respectively and the maximum 5-day rainfall total in each month) and two annually (the number of consecutive dry days and the rainfall amount exceeded only 5% of the time). The driving GCM here was ECHAM5 forcing the PRECIS RCM.